PLOS CLIMATE

RESEARCH ARTICLE

Tracking and forecasting community responses to climate perturbations in the California Current Ecosystem

Mary E. Hunsicker[1☯*], Eric J. Ward[2☯], Michael A. Litzow[3], Sean C. Anderson[4,5], Chris J. Harvey[2], John C. Field[6], Jin Gao[7], Michael G. Jacox[8,9], Sharon Melin[10], Andrew R. Thompson[11], Pete Warzybok[12]

1 Fish Ecology Division, Northwest Fisheries Science Center, National Marine Fisheries Service, National Oceanic and Atmospheric Administration, Newport, Oregon, United States of America, **2** Conservation Biology Division, Northwest Fisheries Science Center, National Marine Fisheries Service, National Oceanic and Atmospheric Administration, Seattle, Washington, United States of America, **3** Alaska Fisheries Science Center, National Marine Fisheries Service, National Oceanic and Atmospheric Administration, Kodiak, Alaska, United States of America, **4** Pacific Biological Station, Fisheries and Oceans Canada, Nanaimo, British Columbia, Canada, **5** Department of Mathematics, Simon Fraser University, Burnaby, British Columbia, Canada, **6** Fisheries Ecology Division, Southwest Fisheries Science Center, National Marine Fisheries Service, National Oceanic and Atmospheric Administration, Santa Cruz, California, United States of America, **7** Centre for Fisheries Ecosystems Research, Memorial University of Newfoundland, St. John's, Newfoundland, Canada, **8** Environmental Research Division, Southwest Fisheries Science Center, National Marine Fisheries Service, National Oceanic and Atmospheric Administration, Monterey, California, United States of America, **9** Physical Sciences Laboratory, National Oceanic and Atmospheric Administration, Boulder, Colorado, United States of America, **10** Marine Mammal Laboratory, Alaska Fisheries Science Center, National Marine Fisheries Service, National Oceanic and Atmospheric Administration, Seattle, Washington, United States of America, **11** Southwest Fisheries Science Center, National Marine Fisheries Service, National Oceanic and Atmospheric Administration, La Jolla, California, United States of America, **12** Point Blue Conservation Science, Petaluma, California, United States of America

☯ These authors contributed equally to this work.
* mary.hunsicker@noaa.gov

OPEN ACCESS

Citation: Hunsicker ME, Ward EJ, Litzow MA, Anderson SC, Harvey CJ, Field JC, et al. (2022) Tracking and forecasting community responses to climate perturbations in the California Current Ecosystem. PLOS Clim 1(3): e0000014. https://doi.org/10.1371/journal.pclm.0000014

Editor: Wei Yu, Shanghai Ocean University, CHINA

Received: September 27, 2021

Accepted: January 5, 2022

Published: March 3, 2022

Peer Review History: PLOS recognizes the benefits of transparency in the peer review process; therefore, we enable the publication of all of the content of peer review and author responses alongside final, published articles. The editorial history of this article is available here: https://doi.org/10.1371/journal.pclm.0000014

Data Availability Statement: All time series collected through the CalCOFI and RREAS surveys are available through the ERDDAP data server (https://coastwatch.pfeg.noaa.gov/erddap/index.html). The seabird and sea lion time series or

Abstract

Ocean ecosystems are vulnerable to climate-driven perturbations, which are increasing in frequency and can have profound effects on marine social-ecological systems. Thus, there is an urgency to develop tools that can detect the response of ecosystem components to these perturbations as early as possible. We used Bayesian Dynamic Factor Analysis (DFA) to develop a community state indicator for the California Current Ecosystem (CCE) to track the system's response to climate perturbations, and to forecast future changes in community state. Our key objectives were to (1) summarize environmental and biological variability in the southern and central regions of the CCE during a recent and unprecedented marine heatwave in the northeast Pacific Ocean (2014–2016) and compare these patterns to past variability, (2) examine whether there is evidence of a shift in the community to a new state in response to the heatwave, (3) identify relationships between community variability and climate variables; and (4) test our ability to create one-year ahead forecasts of individual species responses and the broader community response based on ocean conditions. Our analysis detected a clear community response to the marine heatwave, although it did not exceed normal variability over the past six decades (1951–2017), and we did not find evidence of a shift to a new community state. We found that nitrate flux through the base of the

points of contact are available through the California Current Integrated Ecosystem Assessment (CCIEA) web dashboard (https://www.integratedecosystemassessment.noaa.gov/regions/california-current). The data is third-party data and the authors had no special access or privileges that others would not have.

Funding: Funding for this project came from NOAA's Fisheries and the Environment (FATE) program (project 16-01) awarded to M.E.H, E.J.W., M.A.L. and C.J.H. and NOAA's California Current Integrated Ecosystem Assessment program (C.J. H.). The funders had no role in study design, data collection and analysis, decision to publish, or preparation of the manuscript.

Competing interests: The authors do not have any competing interests (financial or non-financial) with respect to the work presented in this research article.

mixed layer exhibited the strongest relationship with species and community-level responses. Furthermore, we demonstrated skill in creating forecasts of species responses and community state based on estimates of nitrate flux. Our indicator and forecasts of community state show promise as tools for informing ecosystem-based and climate-ready fisheries management in the CCE. Our modeling framework is also widely applicable to other ecosystems where scientists and managers are faced with the challenge of managing and protecting living marine resources in a rapidly changing climate.

Introduction

Climate perturbations can have strong impacts on ocean ecosystems that in turn affect social and economic components of human communities. These effects may be exacerbated when changes in ocean conditions are more extreme, such as during marine heatwaves (prolonged events of anomalously warm ocean waters). The increasing attention on these extreme events and their impacts (e.g., [1, 2]) has invigorated a push for tools that can track and detect as early as possible the response of marine communities to climate-driven perturbations. Early detection, and moreover, near-term forecasts of community shifts could help scientists, managers, and stakeholders better prepare for and respond to the potential consequences of such shifts.

Climate-driven shifts in community structure tend to involve rapid change across multiple populations that result in switches between contrasting community assemblages that may then persist for decades. A growing number of studies have documented community reorganizations in response to climate drivers (e.g., [3–7]). One of the best-known examples is the widespread northeast Pacific community reorganization that followed the 1976/1977 shift in the Pacific Decadal Oscillation from a cold to warm regime [8, 9]. The abrupt change from a cool to warm ocean regime had dramatic implications on ecosystem functioning and living marine resources (LMRs) throughout the region [7, 10–12]. Since then, northeast Pacific marine ecosystems have experienced several interannual or decadal perturbations that do not appear to have resulted in community-wide shifts of similar magnitude.

However, between 2014 and 2016 these ecosystems experienced a marine heatwave that involved the warmest sea surface temperature (SST) and heat content anomalies that had ever been observed over large areas of the North Pacific, with SST anomalies over 6˚C [13, 14]. It was one of the most extreme heatwaves globally in its combined magnitude, spatial scale, and duration [1, 2], and the intense, persistent warming has been attributed to a combination of natural and anthropogenic forcing [15, 16]. Several studies have documented myriad biological responses to this event. For example, within the California Current Ecosystem (CCE), there were mass strandings of marine mammals [17], increased whale entanglements due to shifting prey sources [18], mass mortality events for marine seabirds [17, 19, 20], a record-breaking domoic acid outbreak [21], shifts in pelagic macronekton and micronekton communities and species richness [22–24], irruptions of previously rare fishes and invertebrates throughout the California Current [25–28], and extraordinarily high recruitment of rockfishes (genus *Sebastes*) [29, 30] and northern anchovy (*Engraulis mordax*) [31]. Yet, to date, there have been few quantitative studies of how the marine heatwave impacted the broader CCE community at multiple trophic levels, and therefore the importance of this extreme event for community-wide patterns of variability, and the persistence of the community response, remains largely unknown.

Indicators of community or ecosystem state are valuable tools for tracking climate-related changes in ecosystem functioning and evaluating those changes within the context of past climate perturbations [32]. Moreover, combining long-term monitoring surveys and data with modeling frameworks that summarize information across taxa and life stages that respond quickly to climate perturbations could provide early detection of an ecosystem shifting into a novel state. Early detection of such shifts would benefit ecosystem-based and climate-ready fisheries management strategies aimed at mitigating possible deleterious ecological and socio-economic outcomes. There is also a pressing need for forecasts of future ecosystem states to support forward-looking management of LMRs [33–35], including assessments of risk. As climate models and forecasts of ocean conditions continue to improve, there are burgeoning opportunities to develop and test methods that could provide near-term forecasts of community state in relation to ocean conditions.

A challenge in summarizing ecosystem responses to perturbations is that time series used to characterize the ecosystem often involve tens to hundreds of variables (species or climate indices); there is often some degree of asynchrony among time series (unevenly or irregularly spaced), and further, each is corrupted by the presence of observation errors. Disentangling these sources of error and separating the signal from the noise is statistically challenging. Traditionally, tools such as Principal Components Analysis (PCA) or nonmetric multidimensional scaling have often been used for identifying leading patterns of variability in multivariate datasets (e.g., [36, 37]); however, these approaches are ill-suited to the analysis of time series data that are autocorrelated or non-stationary [38]. An alternative approach, Dynamic Factor Analysis (DFA), is better suited for identifying shared trends that can be used as a community state indicator. DFA is specifically designed for time series ordination, and avoids many of the problems associated with other multi-variate approaches [39]. When applied to a collection of multivariate time series, inference in DFA models focuses on estimating a smaller number of temporal patterns ('trends') that best capture the variation observed. The observed data are then treated as a mixture of these trends [40]. Ward et al. [40] recently developed a Bayesian implementation of DFA that offers added flexibility in model aspects over conventional approaches; examples include allowing for extreme "black swan" events (rare and difficult to predict events) [41] and trend processes that do not follow a random walk. Output from these Bayesian DFA models can also be used to estimate the probability of extreme events occurring or switches among contrasting system states. In the first application of this new method, Litzow et al. [42] examined shared trends of climate and biology time series in the Gulf of Alaska. Their study did not detect evidence for wholesale community reorganization during the recent northeast Pacific marine heatwave; however, their findings indicated potential for new patterns of ecosystem functioning with continued warming of ocean temperatures.

The goal of our study is to build on this set of novel statistical tools to develop a model of the CCE state that can both track and forecast ecosystem changes in response to climate perturbations. More specifically, we expand the Bayesian implementation of DFA to test the community response to environmental variables within the modeling framework and to develop near-term forecasts of future community states. Using climate and biological data from the central and southern regions of the CCE, our specific objectives were to: (1) summarize environmental and biological variability during 2014–2016 marine heatwave and compare these patterns to past variability; (2) examine whether there is evidence of departures from previous climate patterns and of switches to a new community state during the heatwave; (3) identify relationships, if any, between community variability and climate variables; and (4) test our ability to create one-year ahead forecasts of species responses and the community state based on environmental information. While the focus of our study is the CCE, the approach applied

here is widely applicable to the myriad marine ecosystems worldwide that are vulnerable to a rapidly changing climate.

Methods

Data

In our analysis, we used oceanographic time series from the southern (n = 6) and central (n = 6) regions of the CCE, derived from a data assimilative configuration of the Regional Ocean Modeling System (ROMS) with 0.1˚ (~10 km) horizontal resolution and 42 terrain-following vertical levels (oceanmodeling.ucsc.edu) [43]. From the ROMS output, we generated monthly time series covering 1980–2018 for a suite of variables including sea surface temperature (SST), sea surface height (SSH), isothermal layer depth (ILD), Brunt-Väisälä frequency (BV), a coastal upwelling transport index (CUTI), and a biologically effective upwelling transport index (BEUTI). The ILD is similar to mixed layer depth and defines the depth where temperature deviates by 0.5˚C from the surface value. BV is a measure of water column stratification, averaged over the upper 200 m of the water column. CUTI and BEUTI are upwelling indices that quantify vertical transport and nitrate flux through the base of the mixed layer, respectively [44]. The data were annually averaged (July-June) from the coast to 100 km offshore, with the exception of CUTI and BEUTI, which capture coastal upwelling within 75 km of shore. In the alongshore direction, we calculated averages for two regions with a division at Point Conception, California, separating the southern portion of the CCE (31–34.5˚N) from the central region (34.5–40.5˚N, Fig 1). This is in response to the recognition of Point Conception as a major biogeographic boundary for the California Current System, with differing wind and current patterns north and south of that feature [45, 46]. The annual averages were taken from July to June to capture the influence of the El Niño–Southern Oscillation (ENSO), which peaks in winter and is the dominant mode of interannual variability influencing the California Current [47]. We developed models using ROMS output rather than empirical measurements because they provide full spatial and temporal coverage of surface and subsurface conditions, incorporate available observations, and will enable the use of ROMS forecasts to then forecast biological changes in the CCE. This ocean model is constrained by available satellite and *in situ* observations to improve its fidelity to nature and has been validated against independent *in situ* observations [43, 48]. Output from this model has been widely used to characterize CCE oceanography, its relation to large scale climate variability, and its influence over the marine ecosystem from phytoplankton to top predators (see Discussion). More details on the oceanographic time series can be found in S1 Table and S1 Fig.

The biology time series included in our analysis were selected based on three criteria: first, the measured variables would be expected to show rapid (0- to 1-year lag) responses to climate variability; second, the time series could be updated with no more than one year lag for processing time to increase the speed at which biological responses to perturbation could be detected; and third, the time series were at least 15 years long. A threshold of 15 years allowed us to include long time series that spanned as many climate perturbations as possible and also have enough biological time series to develop an informative indicator of community state. In addition, 15 years is a threshold that has been previously used to define "long oceanographic time series" in the California Current [50]. The biology time series that met our selection criteria (n = 38) included ichthyoplankton, pelagic young-of-the-year (juvenile fish), squid, and krill abundance; seabird productivity; and California sea lion pup body condition metrics (S1 Fig, S1 Table). These 38 time series were collected from four disparate ocean surveys, and span between 22 and 68 years. Datasets collected from surveys that included spatial attributes (e.g., ichthyoplankton and pelagic juvenile fish surveys) were first standardized using Generalized

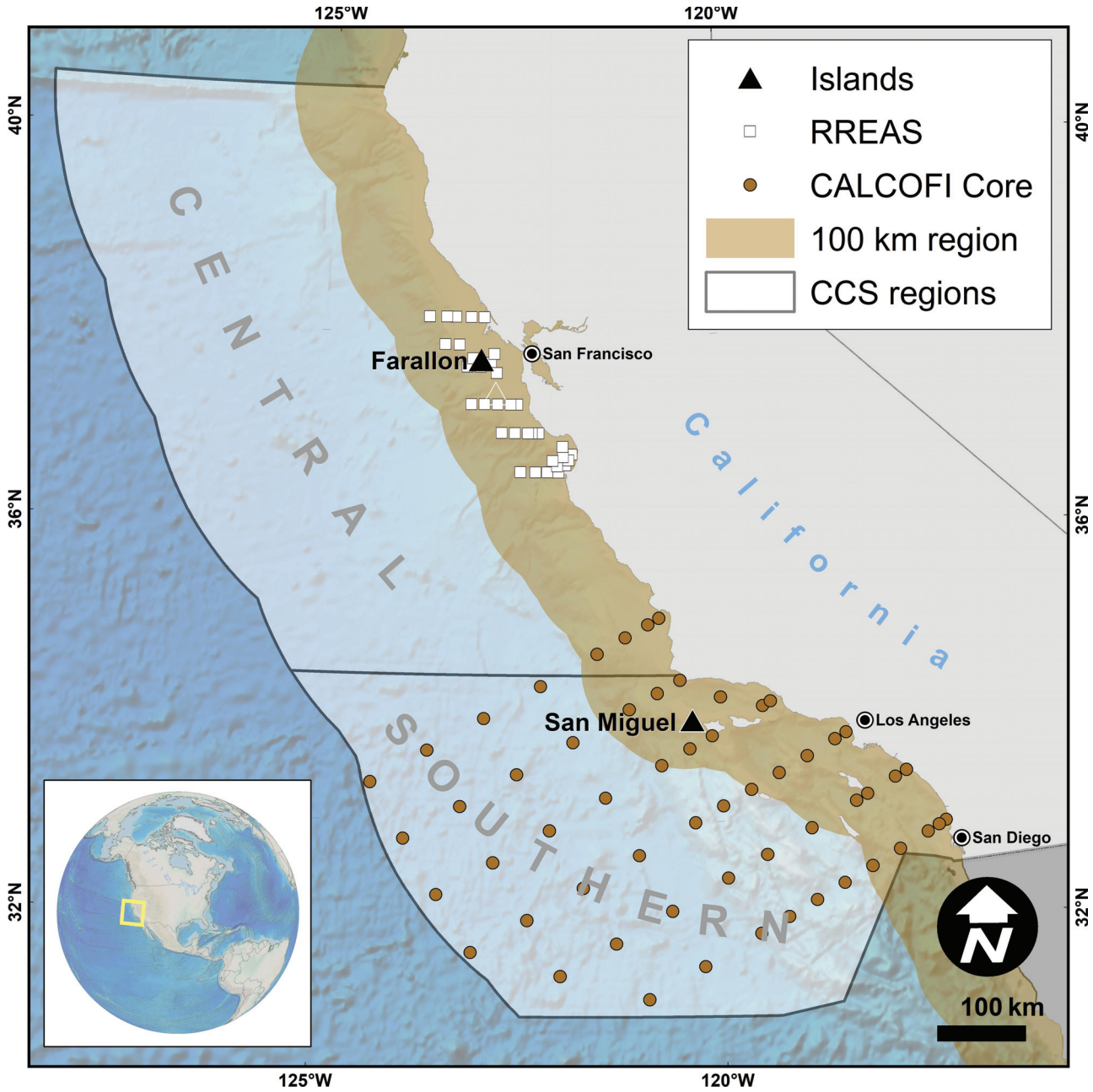

Fig 1. Sampling locations of California Current Ecosystem biology included in the study analyses. Abundance data for pelagic juvenile groundfishes and invertebrates are collected on the Rockfish Recruitment and Ecosystem Assessment Survey (RREAS). Ichthyoplankton data are collected on the California Cooperative Oceanic Fisheries Investigations (CalCOFI) survey. Seabird reproductive success and California sea lion (*Zalophus californianus*) pup time series are collected on Southeast Farallon Island and San Miguel Island, respectively. See S1 Table and S1 Fig for detailed information on the individual time series. The base map layer was sourced from NOAA National Geophysical Data Center (2009) ETOPO1 1 Arc-Minute Global Relief Model. NOAA National Centers for Environmental Information (accessed: 19 April 2013, [49]).

https://doi.org/10.1371/journal.pclm.0000014.g001

Additive Models to create a univariate time series for each species. While these datasets generally include spatial random sampling, the index standardization accounts for uneven distributions of effort (in space or time). Details on the standardization of individual datasets are included in S1 Appendix. In addition, the biology data were normalized with log transformations where appropriate (all zeros were changed to NAs). For example, if the time series data

were assumed to be lognormally distributed (e.g., weight/count data) or the coefficient of variation was > 1, the data were log transformed. All of the time series from an individual dataset (survey) were treated the same, i.e., logged or not. More details on the biology time series used in this study and the associated data sources and log transformations are summarized in S1 Table.

Modeling

We describe the methods in detail below, but in summary our work flow was to (1) apply Bayesian DFA to climate and biology datasets separately and use model selection tools to identify the best supported model and number of shared trends, (2) apply 'black swan' and regime detection methods to detect extreme events and alternating community states, respectively, (3) identify whether the CCE community state was strongly correlated with the climate time series (compare performance of the biology models with/without environmental covariates), and (4) evaluate our skill at making predictions of community state and individual species variables. These four steps map on to the four study objectives outlined in the introduction.

Dynamic factor analysis

We used a Bayesian version of Dynamic Factor Analysis (DFA) [39, 40] using the software Stan and R [51, 52] as implemented in the 'bayesdfa' package [53]. DFA is a multivariate statistical tool somewhat analogous to Principal Components Analyses, but for time-series data (https://cran.r-project.org/web/packages/MARSS/vignettes/UserGuide.pdf) [54]. For a collection of time series, the number of estimated 'trends' is specified *a priori*, and DFA estimates these latent trends as independent random walks. In mathematical form, this is expressed as

$$\boldsymbol{x_t} = \boldsymbol{x_{t-1}} + \boldsymbol{w_{t-1}},$$

where $\boldsymbol{x_t}$ represents the value of latent (unobserved) trends at time t, and the process error deviations $\boldsymbol{w_{t-1}}$ are generally assumed to be white noise having arisen from a multivariate normal distribution (with an identity covariance matrix for identifiability). The latent trends are mapped to the observed data through an estimated loadings matrix $\mathbf{Z}$ and residual error $\boldsymbol{e_t}$,

$$\boldsymbol{y_t} = \mathbf{Z}\boldsymbol{x_t} + \boldsymbol{b} \cdot \boldsymbol{d_t} + \boldsymbol{e_t},$$

where $\boldsymbol{y_t}$ is the vector of observed states at time t, and the residual error terms $\boldsymbol{e_t}$ are assumed to be drawn from a univariate or multivariate normal distribution. Though the covariance matrix of $\boldsymbol{w_t}$ is generally fixed [39], the covariance matrix of $\boldsymbol{e_t}$ can be structured; variances may be shared or not across time series, and off diagonal elements may be estimated. The parameter vector $\mathbf{b}$ represents optional estimated coefficients relating covariates $\boldsymbol{d_t}$ to the observed response. In the context of our DFA modeling, we included climate variables as $\boldsymbol{d_t}$ in models where the biological observations were used as the response $\boldsymbol{y_t}$.

Because we implemented the DFA model in a Bayesian setting, we were able to extend this model to include additional features. First, to include extreme events, we relaxed the assumption about process errors $\boldsymbol{w_t}$ being drawn from a normal distribution and used a multivariate Student-t distribution (MVT) instead [55]. We also modified the process equation to consider an optional vector of AR(1) coefficients $\boldsymbol{\phi}$ on the latent trends. $\boldsymbol{x_t} = \boldsymbol{\phi x_{t-1}} + \boldsymbol{w_{t-1}}$ [40]. A final modification of the conventional DFA model is that for some models, process variances can be estimated rather than fixed at 1 (maximum likelihood approaches generally use this constraint for identifiability). As implemented in Stan [51, 56, 57], we conducted estimation with three chains, with a warm-up of 2000 samples, followed by 2000 iterations. We used the split-chain potential scale reduction factor [58, 59] to assess convergence (Rhat < 1.05). Code to replicate

these analyses is deployed as an R package on CRAN ('bayesdfa') [53] and our public GitHub repository, https://github.com/fate-ewi/bayesdfa.

Models structure optimization

We ran the DFA on climate datasets (1981–2017) and biological datasets (1951–2017) across the southern and central regions of the California Current combined. Running the analysis at this spatial scale allowed us to capture the broader community response to climate perturbations, compared to running models on each multivariate dataset independently (e.g., time series from a single survey). There are a number of ways to evaluate predictive accuracy of these models. The commonly used Leave-One-Out Cross-Validation (LOO-CV), for example holds each observation out in turn and predictions are made from the remaining data. As our focus was on the temporal nature of the data and forecasting component, we implemented a variant of k-fold cross validation and treated individual years as unique 'folds'. Because our objectives involved evaluating these models for future predictions, we implemented the Leave-Future-Out Cross Validation Information Criterion (LFO-CV) [60]. We used this approach to identify data support for (1) the number of latent DFA trends (n = 1–3), (2) first-order autoregressive AR(1) coefficients on the trends (ϕ estimated with a Normal(0,1) prior), (3) Student-t deviations (i.e., evidence of extreme events, using a prior on the MVT degrees of freedom parameter, ν, of $\nu \sim$ Gamma(2, 0.1)), and (4) a fixed versus estimated trend variance (using a prior on the standard deviation, σ_w, of $\sigma_w \sim$ Normal(0, 1)).

In addition, we used LFO-CV to identify the most appropriate error structure for the climate dataset—specifically whether the times series had equal (shared) or unequal (unique) observation errors. For the biology models, we assumed the observation errors were unique by dataset, and our estimates of survey variance supported this assumption.

For each model formulation, we applied the LFO-CV method by first fitting the model to all years of data prior to year T (i.e., training data, years 1, 2, . . ., (T-1)) and then using the fitted model to predict the trend value in year T (i.e., test data). We repeated this process for 10 years, starting with 2017 as year T and working back to 2008, and then calculated the expected log predictive density (ELPD) across those time steps. The climate and biology models with the highest ELPD were deemed the best supported models. The LFO-CV is a preferred method for evaluating future predictive performance of Bayesian models because it properly accounts for time series structure, and unlike other Bayesian cross-validation methods, does not produce overly optimistic estimates [60].

Detection of extreme events and regime shifts

After identifying the best-supported DFA model for the climate and biological datasets, we conducted a post-hoc examination of outlier detection and regime shifts. For outlier detection of black swan events, we implemented a method similar to that described in Anderson et al. [41] and applied it to the climate and biology time series. This approach relies on first differencing the posterior trend mean estimates of the climate and biology trends, $\boldsymbol{x}_t - \boldsymbol{x}_{t-1}$ and then applies a normal density function to identify year-over-year changes that were unlikely to have arisen from a normal distribution (given the process variance). Probabilities can then be assigned to the deviations in each year (e.g., 'there is a 1:1000 chance of observing a deviation similar to that estimated in year t'). As described in Ward et al. [40], the presence of regimes can also be estimated by applying hidden Markov models (HMM) to the estimated state indices from a DFA. We evaluated support for regimes and alternate states by using the posterior trend estimates from each model as input. The Bayesian Leave-One-Out Cross Validation

information criterion (LOO-CV) [61] was used to identify the data support for the number of regimes (n = 1–3). The model with the lowest LOO-CV value is deemed the best model.

Climate-biology relationships and forecasts of community state

While a wide variety of multivariate or univariate time series methods could be applied to our observed time series to generate forecasts, our objectives were to develop simultaneous estimates of both the community state (i.e., the DFA trend value) and the raw time series (i.e., individual time series summarized by the biology DFA model). We evaluated the ability of our DFA models to generate short-term (one year lead-time) forecasts of community state by first evaluating whether the performance of the biology DFA model was improved when climate time series were included as covariates in the model. If climate time series were found to better explain the variability in the biology time series, these relationships could potentially be used to forecast community trends. For our analysis, we ran the DFA on a subset of the biology data overlapping in time with the climate dataset, i.e., 1981–2017, to make out-of-sample predictions. We used the same LFO-CV procedure described above, with the same forecast period (2009–2017) to compare the biology models with and without a single climate covariate (see S2 Table for all model formulations). In this case, the model used biological and climate data from all preceding years and climate data from the year to be forecast. The six climate covariates from the southern region and the central region of the CCE (12 total) were tested in this analysis. Once the best-supported biology-covariate model was identified, we used that model to make predictions of the community state (i.e., DFA trend value) in 2018 using climate data from that same year and the raw time series of the individual species (i.e., the biology time series summarized by the DFA model). We evaluated forecast skill based on the prediction errors of individual species time series and by comparing the forecasts for 2008–2018 to the 2008–2018 trend values estimated from the biology-covariate model that only included data prior to the forecast year.

Results

Climate and biology trends

The model with the highest predictive accuracy (ELPD) of the climate state in the southern and central regions of the CCE was a one-trend DFA model (Model 1 in Table 1, Fig 2). This model included unique observation variances across the six time series, support for heavy-tailed deviations of the latent trend, an AR(1) coefficient on the trend (S2 Fig), and an estimated trend variance. Overall, the trend captured a well-documented cooling period in the CCE between 1980 and 2010 (e.g., [62]) as well as strong El Niño events (e.g., 1982–1983, 1997–1998, 2015–2016) and the 2014–2016 marine heatwave. The trends and loadings indicate that these events were generally associated with weaker upwelling, reduced mixed layer depth, low nutrient flux, and warm, stratified waters (Figs 2 and 3). All but one of the climate time series (central ILD) were strongly associated with the single trend, i.e., at least 90% of the loading posterior distributions associated with each time series were above or below zero (Fig 3). The SST, SSH, and BV frequency (water column stratification) time series from the southern and central regions of the CCE loaded positively on this trend (Fig 3). The BEUTI and CUTI time series from both regions of the CCE and the ILD time series from the central region loaded negatively on the trend (Fig 3).

The climate state during the marine heatwave, as indicated by the DFA trend, was within the bounds of previous observations. While there was support in the best model for heavy-tailed deviations in the climate trend (i.e., Student-t deviations S3 Fig), our post-hoc examination of outliers detected a single extreme event in the climate state in mid-1998 to mid-1999

Table 1. Summary information for climate and biology Bayesian DFA models, including whether process error was estimated, observation error variances (unequal or equal among time series, or unique to each survey), the number of model trends, expected log pointwise predictive densities (ELPD), and standard error of ELPD.

Time series	Model	Process sigma	Variance index	Trends	ELPD	SE ELPD
Climate	1	Yes	unequal	1	**-10551.89**	759.44
	2	No	unequal	1	-10682.39	712.96
	3	Yes	equal	1	-16793.59	1732.54
	4	No	equal	1	-16881.03	1824.42
	5	No	unequal	2	-17441.01	1655.23
	6	Yes	unequal	2	-17818.86	1813.65
	7	Yes	unequal	3	-21571.65	1674.77
	8	No	unequal	3	-22882.99	1695.12
	9	No	equal	2	-23927.86	2694.72
	10	Yes	equal	2	-24536.19	2953.38
	11	Yes	equal	3	-38895.66	4024.93
	12	No	equal	3	-38920.87	4762.15
Biology	13	No	survey	1	**-2003.32**	95.76
	14	Yes	survey	1	**-2003.96**	88.88
	15	No	survey	2	-2155.52	76.05
	16	Yes	survey	2	-2198.79	78.86
	17	No	survey	3	-2334.55	118.31
	18	Yes	survey	3	-2335.10	112.70

Bold text highlights the models that show best support or highest predictive accuracy for the climate and biology data for the southern and central California Current ecosystem (i.e., highest ELPD). All climate and biology models include an AR(1) process and Student-t deviations.

https://doi.org/10.1371/journal.pclm.0000014.t001

(threshold = 0.001), when there was a shift from strong El Niño (1997–98) to strong La Niña (1998–1999) conditions, and not around the time of the heatwave. Application of the Bayesian HMM to the climate trend most supported the presence of two hidden states, reflecting the probability of being in a state associated with warmer conditions versus one with cooler conditions (LOO-CV: one-state = 129.1, two-state = 9.4, three-state = 27.2, Fig 4). The LOO-CV did not provide support for a shift to a third novel climate state in the southern and central regions of the CCE during the marine heatwave, however there is a shift back to the previously observed warm state during the marine heatwave.

The best model for community variability among our biological time series was also a one-trend model (Model 13 in Table 1, Fig 5). The model formulation was similar to the best climate model, except the observation variances were unique by dataset (survey) and not individual time series. We note that the top two models (Model 13 and 14) showed similar predictive accuracy (Δ ELPD < 1) and only differed with respect to whether the process variance was fixed at 1 or estimated. Here we only show results for the model with a fixed process variance. The biology showed strong coherence in community signal; a majority of the time series (31 of 38) loaded strongly (probability > 0.9) on the single trend and most of them demonstrated loadings in the same direction (Fig 6). The magnitude and direction of the estimated loadings were consistent with the observed high relative abundance of most juvenile groundfishes (rockfish, flatfish), squid, krill, and some ichthyoplankton species during the marine heatwave, and suggest that the reproductive success of some seabird species was higher around the time of the heatwave as well. The few time series loading in the other direction on the trend indicated a reduction in sea lion pup growth rate and lower abundances of juvenile/adult Pacific

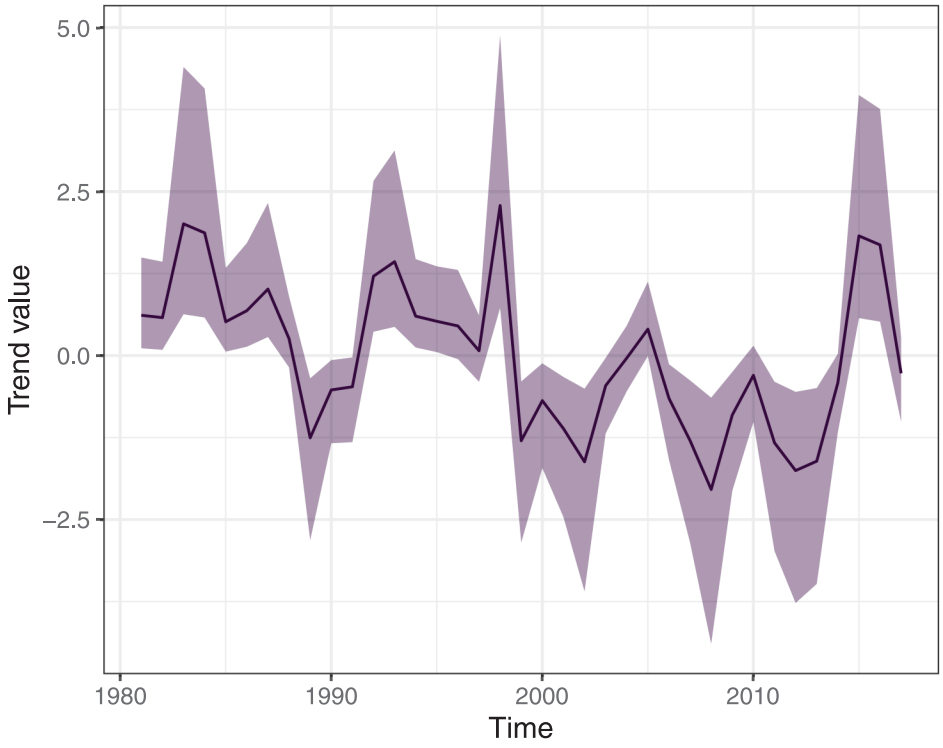

Fig 2. Shared trend with 95% credible intervals of climate variability in the southern and central California Current ecosystem (1981–2017).

https://doi.org/10.1371/journal.pclm.0000014.g002

sardine *Sardinops sagax* and some ichthyoplankton species (e.g., larval northern anchovy and Pacific hake *Merluccius productus*) associated with the heatwave.

The estimated trend from this biology DFA model demonstrates a potential shift in community state in the mid-1960s, although there is considerable uncertainty around the trend during this early portion of the time series, likely due to the limited number of observations (ichthyoplankton only) pre-dating the 1970s (Fig 5, S1 Fig). The community state appears to be relatively stable from the late 1970s through the early 2000s, and the trend reached a peak around 2013–2015. Evidence of a community shift early in the time series is supported by our regime detection analysis, which demonstrated that a two-state model best described the latent trend (LOO-CV: one-state = 216.4, two-state = 11.8, three-state = 41.8, Fig 7). This shift coincides with a strong increase in the abundance of a few species during that period, including eared blacksmelt (*Lipolagus ochotensis*), slender blacksmelt (*Bathylagus pacificus*), northern lampfish (*Stenobrachius leucopsarus*), which are cool water associated mesopelagic species, as well as a rise in northern anchovy (*Engraulis mordax*) abundance prior to the shift (S1 Fig). Our analysis does not document a shift to a novel community state in response to the recent marine heatwave.

While this model provided slight support for heavy-tailed Student-t deviations in the latent trend (S4 Fig), we did not detect any black swan events in the community state. We note that the community response to two strong El Niño events (1982–1983 and 1997–1998) and to unusually low productivity conditions (2005) in the central CCE appear similar in magnitude and duration to the response to the 2014–2016 marine heatwave, although the directions of the responses were opposite (Fig 5). Our regime detection analysis also captured the change in

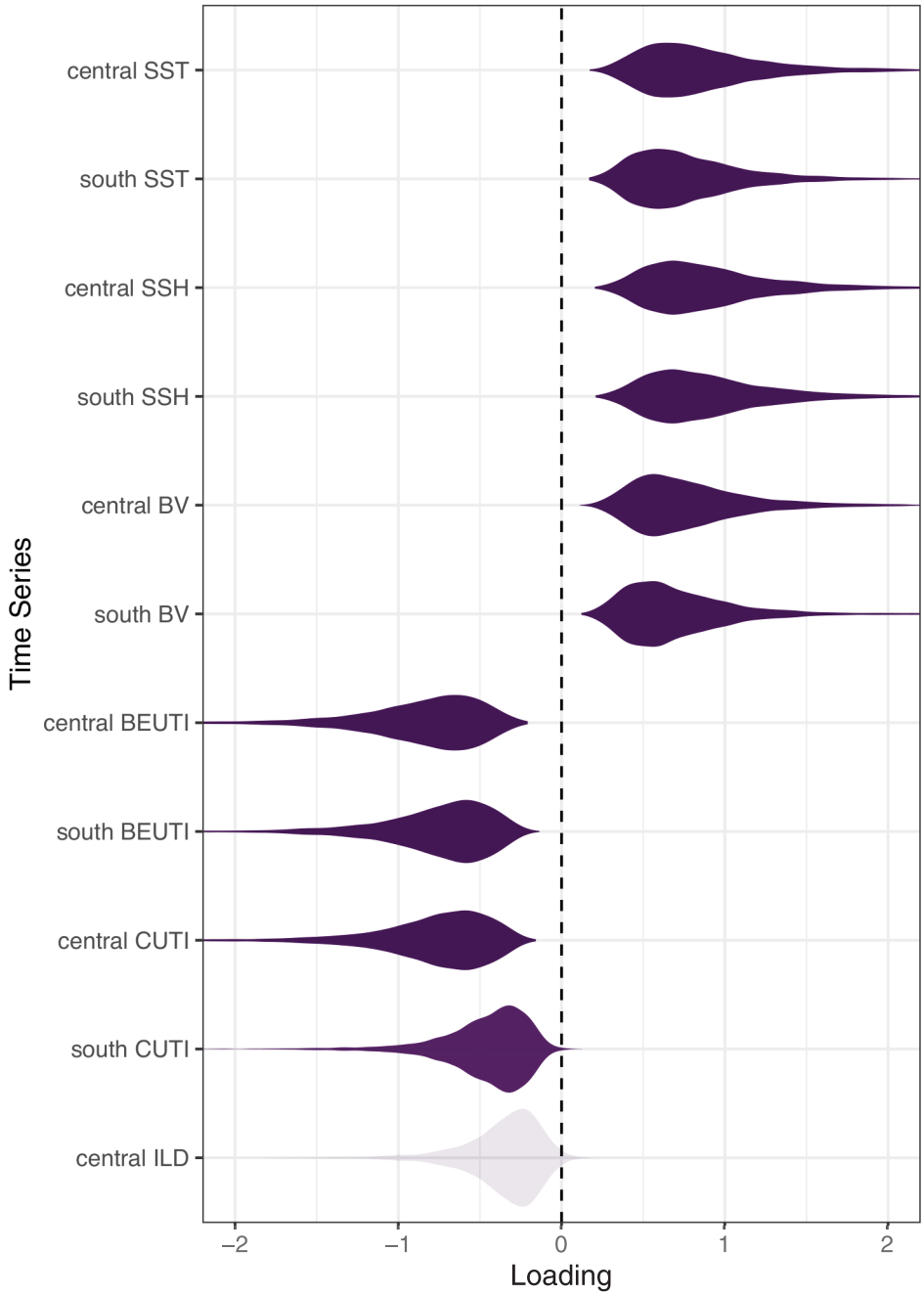

Fig 3. Posterior distributions for loadings on all of the individual time series associated with the climate trend (Fig 2). Loadings with darker shading indicate time series loading most strongly on the climate trend. SST, sea surface temperature; SSH, sea surface height; ILD, isothermal layer depth; BV, Brunt-Väisälä frequency (stratification); CUTI, Coastal Upwelling Transport Index; BEUTI, Biologically Effective Upwelling Transport Index. See S1 Table and S1 Fig for climate times series details.

https://doi.org/10.1371/journal.pclm.0000014.g003

the central CCE community in the mid to late 2000s (Fig 7), which may be associated with the large changes in the reproductive success of multiple seabirds (e.g., Cassin's auklet *Ptychoramphus aleuticus*, common murre *Uria aalge*, Brandt's cormorant *Urile penicillatus*) and in sea lion pup births around that time (S1 Fig). These taxa may have been impacted by changes in

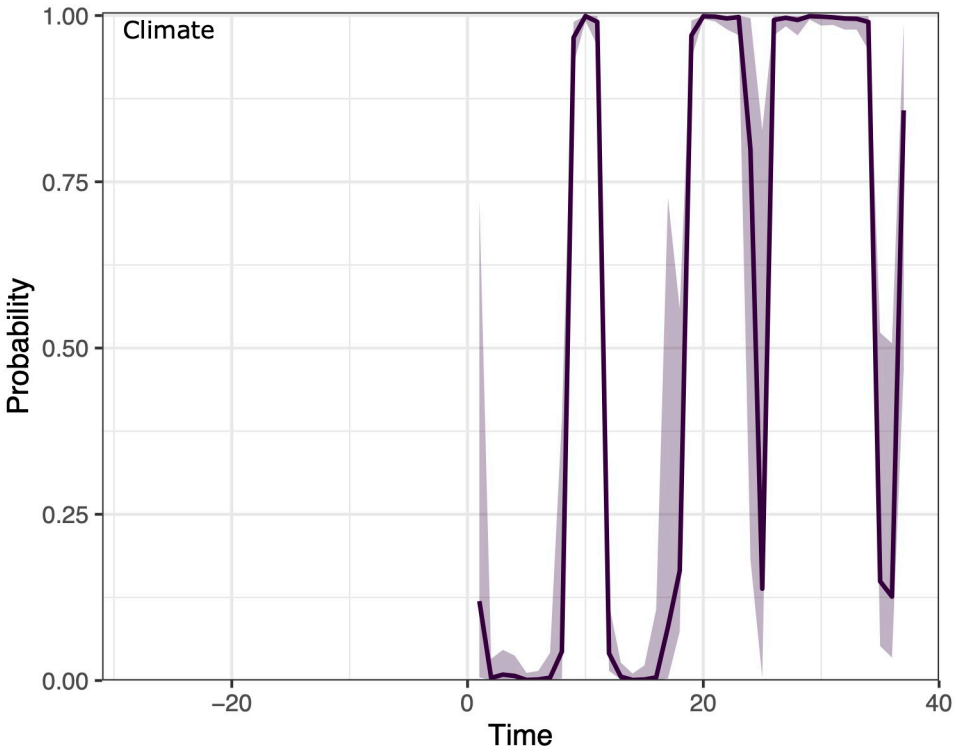

Fig 4. Results of Hidden Markov Models (HMM) showing state probability for latent trends in the climate data set. The best model invoked two states, and the median probability (and 95% credible intervals) of being in one state versus the other is shown. The figure reflects the probability of being in the state associated with warmer conditions versus one with cold conditions.

https://doi.org/10.1371/journal.pclm.0000014.g004

the abundance or availability of important prey items resulting from unproductive ocean conditions in the central CCE in 2005 and the below normal SSTs associated with the 2007–2008 La Niña Event [63–65].

Forecast of community state

In comparing models of the biological response with and without climate covariates, we found that several biology models with climate predictors outperformed the biology models that did not include covariates (S2 Table). The climate covariate resulting in the best future predictions of community state was BEUTI (central region), followed by CUTI (central region) (Table 2, see S2 Table for all models). The coefficients linking BEUTI to observed time series indicate strong, positive relationships between nitrate flux and the reproductive success of seabirds and the abundance of krill in the central California Current (Fig 8). They also indicate strong, negative relationships between nitrate flux and the abundance of juvenile/adult Pacific sardine and larval northern anchovy (Fig 8). The remaining biology-BEUTI relationships were moderate (e.g., ichthyoplankton, market squid *Doryteuthis opalescens*) to weak (e.g., rockfish spp., Fig 8). The biology-CUTI model was similar to the biology-BEUTI model with respect to model structure and estimated species loadings. The estimated coefficients in the CUTI model (S5 Fig) also show a similar pattern to those in the biology-BEUTI model. The remaining covariate models only showed weak climate-biology relationships (e.g., S6 and S7 Figs).

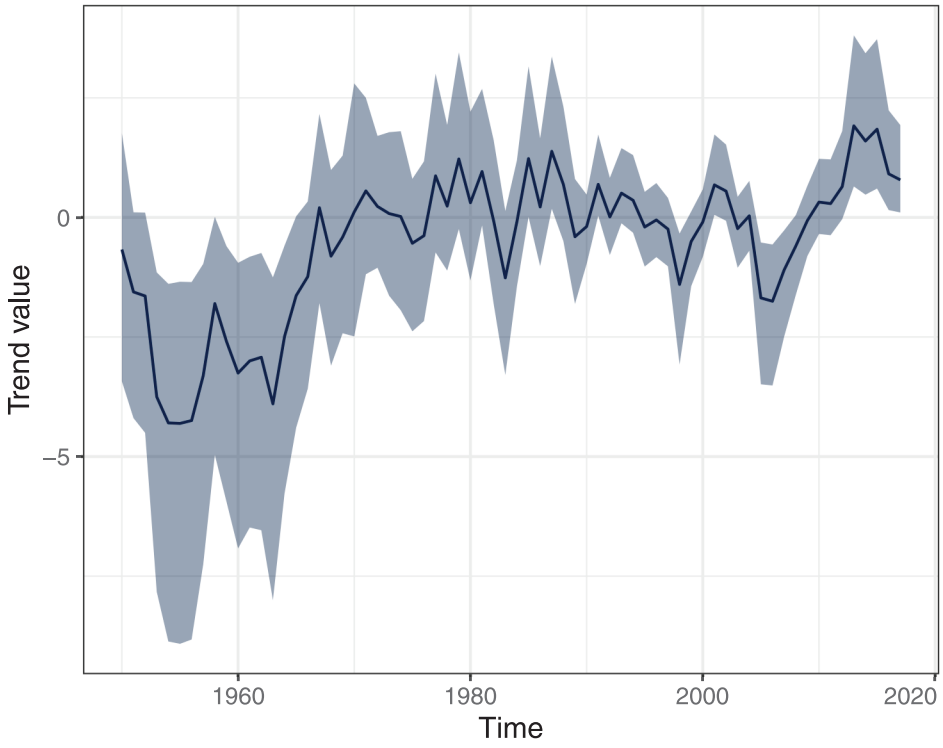

Fig 5. Shared trend with 95% credible intervals of community variability in the southern and central California Current ecosystem (1951–2018: Marine heatwave occurred 2014–2016).

https://doi.org/10.1371/journal.pclm.0000014.g005

Given that the biology-BEUTI model was the best supported model over the null model (a model without covariates), we were interested in evaluating the ability of this covariate model to forecast the community state. Comparisons between the community state and the community state forecasts (out-of-sample estimates) indicate that we had skill in forecasting community state one year in advance (Fig 9). Forecasts of the community trend values for ten additional years (2008–2017, Fig 10) also indicate that we had some skill for many of the years tested. There are wide confidence intervals around the forecasts; however, given our methodology we can expect that the credible intervals around the trend forecast will be larger than the historical credible intervals (Fig 9). Forecasts have more uncertainty than historical values because the variance of a random walk increases linearly with time [66, 67]. Furthermore, our credible intervals are increased because we are additionally (1) propagating full parameter uncertainty across the MCMC draws projecting it, and (2) using a Student-t distribution, which has heavy tails and therefore makes the uncertainty intervals wider than if we used normal distribution.

Overall, the model forecast skill of individual species parameters was moderate to high for half of the species included in the biology-BEUTI model (S3 Table, S9 and S10 Figs). It is important to emphasize that the source of variability in predictions for each of the original time series is a mixture of the magnitude and uncertainty around the trends and loadings ($\boldsymbol{x}_t$, $\mathbf{Z}$), and the magnitude and uncertainty in the estimated covariates ($\boldsymbol{b}$). On the one hand, the time series associated with the highest predictive skill (i.e., lowest prediction errors) included seabird reproductive success (common murre, Cassin's auklet) and the abundance of juvenile Pacific sanddab *Citharichthys sordidus*, juvenile halfbanded rockfish *Sebastes semicinctus*,

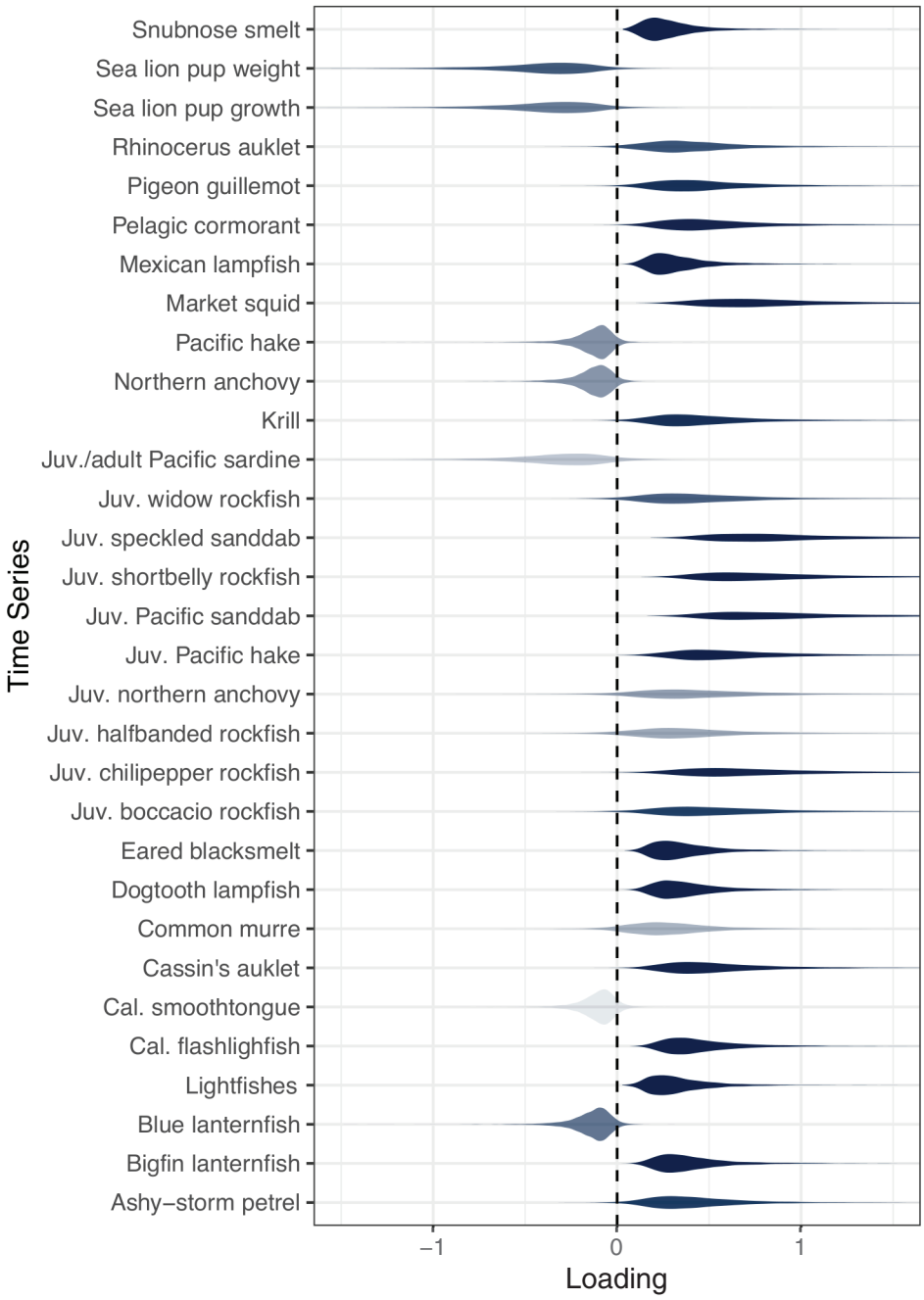

Fig 6. Posterior distributions for loadings on individual time series associated with the biology trend (Fig 5). Only time series with ≥ 90% of the loading distributions above or below zero are shown). Loadings with darker shading indicate time series loading most strongly on the biology trend. Cal. = California, Juv. = juvenile fish stage, Juv./adult = juvenile and adult fish stages combined, all other fish are larval fish. See S1 Table and S1 Fig for times series details.

https://doi.org/10.1371/journal.pclm.0000014.g006

market squid, and several ichthyoplankton species (S3 Table, S9 and S10 Figs). On the other hand, forecast skill was lowest (i.e., highest prediction errors) for the abundance of some juvenile rockfishes (chilipepper *Sebastes goodei* and widow rockfish *Sebastes entomelas*) and larval fishes (northern anchovy, mesopelagics), which is likely attributed to a lag or mismatch in the

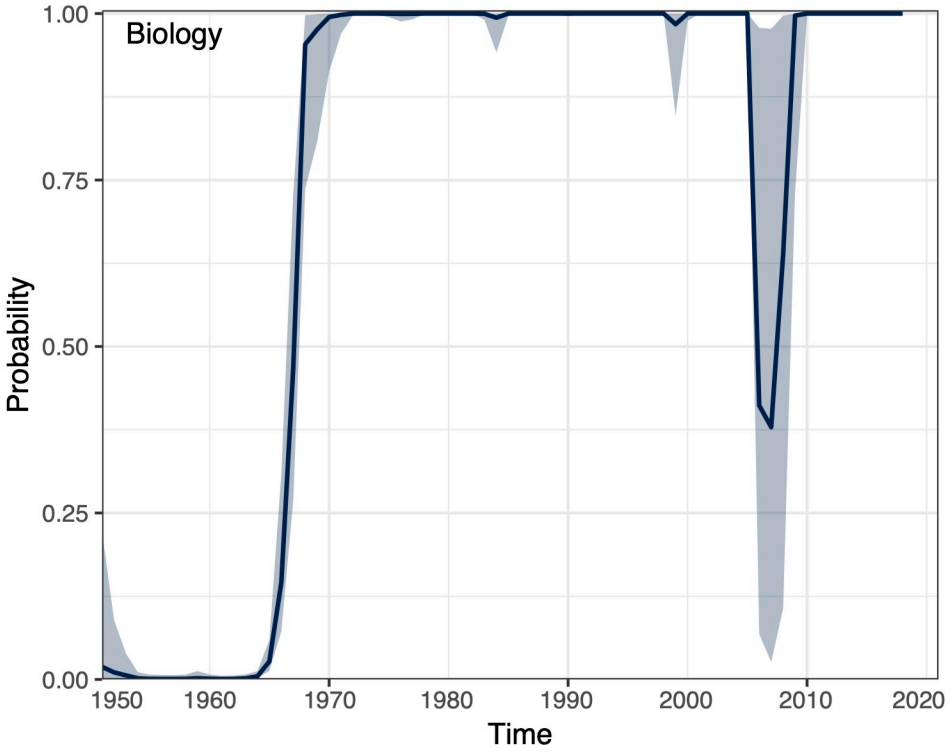

Fig 7. Results of Hidden Markov Models (HMM) showing state probability for latent trends in the biology data set. The best model invoked two states, and the median probability (and 95% credible intervals) of being in one state versus the other is shown. The figure indicates that ecosystem did not shift into a new state following the marine heatwave.

https://doi.org/10.1371/journal.pclm.0000014.g007

timing of the climate-biology relationships. These patterns in forecast skill are similar to those based on the biology-CUTI, -SST, and -ILD models (S3 Table). Lastly, the uncertainty around model predictions of species parameters appears to be driven more by the precision of the model coefficients than by the loadings on the community trend (e.g., S11 Fig).

Table 2. Summary information for the top biology-covariate Bayesian DFA models for each covariate and the top two biology only models (years 1981–2017).

Model	Process sigma	Trends	ELPD	SE ELPD	Covariate	Region
1	**No**	**1**	**-1878.71**	**71.52**	**BEUTI**	**central**
2	No	1	-1905.27	81.98	CUTI	**central**
3	No	1	-1914.62	83.22	ILD	south
4	No	1	-1927.33	88.26	SST	south
5	No	1	-1928.03	88.39	BV	south
6	No	1	-1946.75	86.33	SSH	south
7	No	1	-1951.44	73.59	None	-
8	Yes	1	-2038.71	91.44	None	-

The table indicates whether process error was estimated ('Yes') or fixed ('No'), the number of model trends, expected log pointwise predictive densities (ELPD), standard error of ELPD, the environmental covariate included in the model, and the region in the California Current over which the covariate was aggregated. All models had an AR(1) coefficient on the trend and Student-t deviations. Model 1 was deemed the best model based on its highest predictive accuracy (highest ELPD value) compared to all other models. BEUTI = Biologically Effective Upwelling Transport Index; BV = Brunt-Väisälä frequency; CUTI = Coastal Upwelling Transport Index; ILD = Isothermal Layer Depth; SST = Sea Surface Temperature; SSH = Sea Surface Height. See S2 Table for the full suite of model comparisons.

https://doi.org/10.1371/journal.pclm.0000014.t002

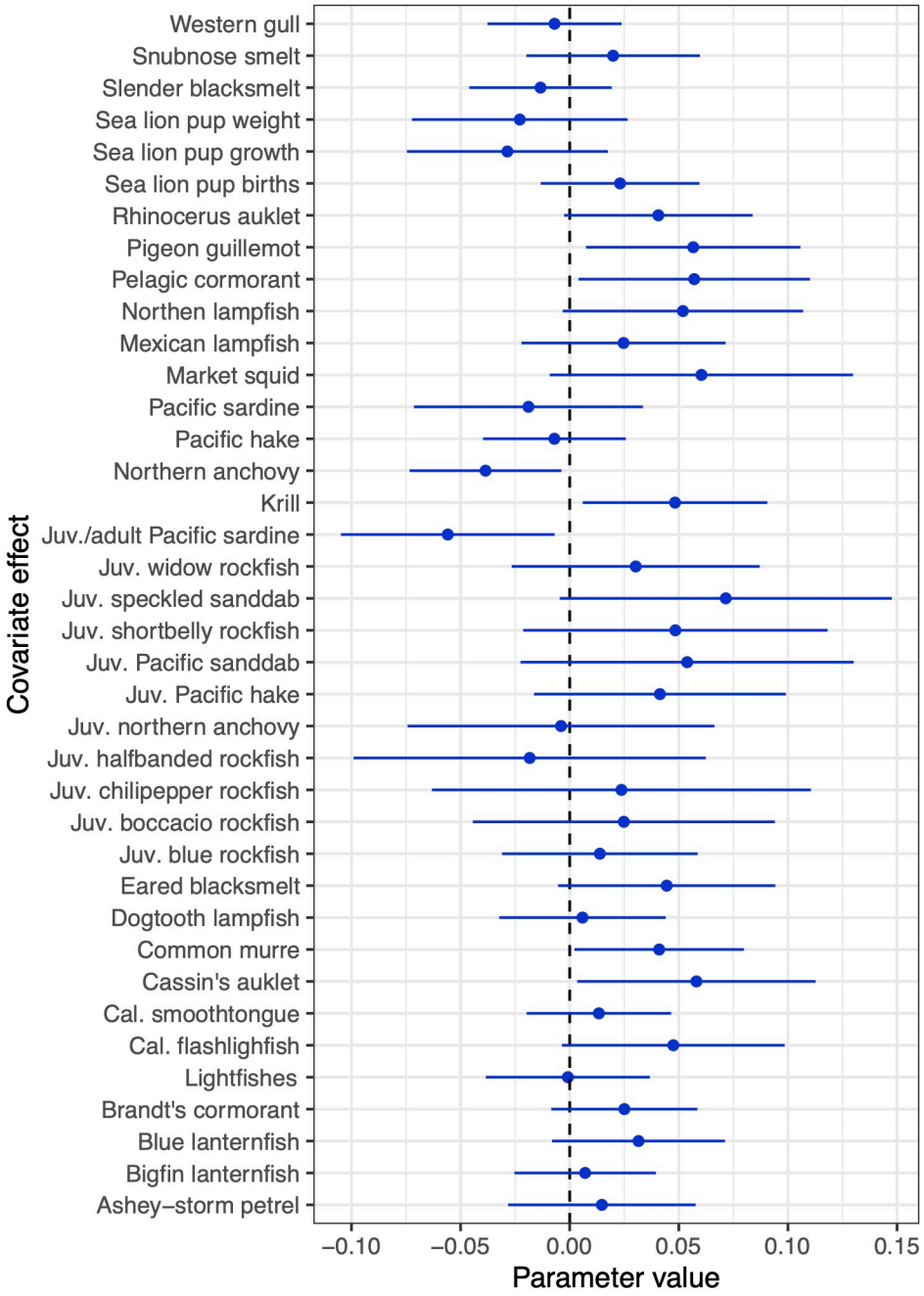

Fig 8. A summary of the effect of the Biologically Effective Upwelling Transport Index (BEUTI), a measure of nitrate flux through the base of the mixed layer, on the single species parameters. Cal. = California, Juv. = juvenile fish stage, Juv./adult = juvenile and adult fish stages combined, all other fish are larval fish. Blue error bars reflect 95% credible intervals. S5–S7 Figs show effects of other environment covariates on the biological variables.

https://doi.org/10.1371/journal.pclm.0000014.g008

Discussion

We applied a novel set of statistical tools to data from the southern and central regions of the CCE to document the community response to climate perturbations over the past six decades and to create near-term forecasts of community state. Our analysis detected a community response to the 2014–2016 northeast Pacific marine heatwave; however, it did not exceed

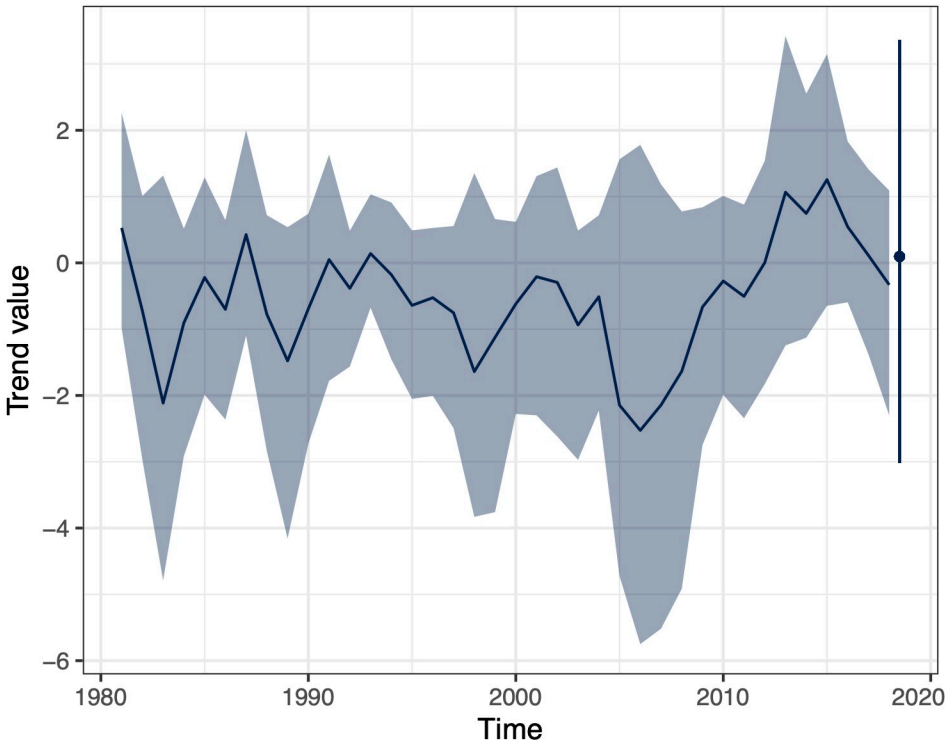

Fig 9. Community variability and forecast of the community state in the southern California Current. The shared biology trend (blue line, with 95% credible intervals) derived from biology-BEUTI model fit to subset of data (1981–2018) is shown along with the trend forecast for 2018 (circle, with 95% credible intervals). See S8 Fig for model loadings.

https://doi.org/10.1371/journal.pclm.0000014.g009

normal variability within the study timeframe or result in a shift to a novel community state, based on the biological time series investigated here. We identified relationships between community state and multiple climate variables, with nitrate flux through the base of the mixed layer having the strongest correspondence with individual species time series and the shared trend in community variability. Moreover, we demonstrated skill in creating simultaneous one-year lead time forecasts of species responses and community state.

Long-term changes in community state

Many studies and anecdotal accounts have documented unexpected biological responses to the 2014–2016 northeast Pacific marine heatwave. Based on the biological time series included in our analysis, the broader CCE community demonstrated a clear response to the marine heatwave (Fig 5). However, our results do not demonstrate a widespread community reorganization beyond the archetypal community structure of this dynamic ecosystem in response to this event. Instead, the mean values for the shared trend in the biology time series, as well as for the shared climate trend, were within the range of previous observations. Many species were present during the marine heatwave that are not typically observed in the CCE. While our analysis could not include these sporadically occurring taxa, due to the large number of zero observations in the historic survey data, the exceptional presences and high abundances of those warm species did not result in a persistent signal among the species included in the DFAs. As additional years of data become available, the DFA models could reveal different outcomes from 2014–2016. However, this is unlikely given that the taxa and life stages used in

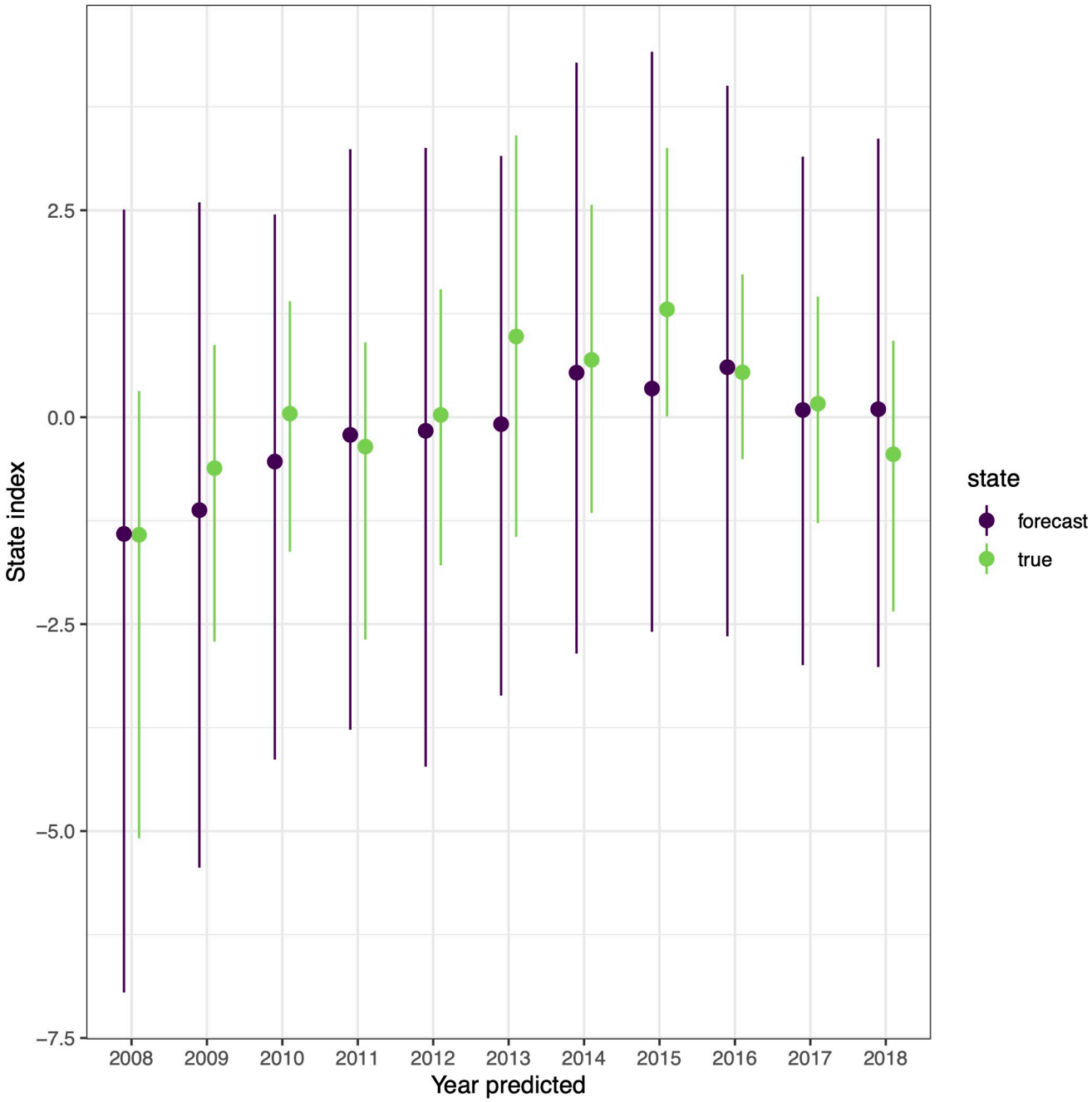

Fig 10. Forecasts and model estimates of the 'true' community state in the southern and central California Current in years 2008–2018 (circle, with 95% credible intervals).

https://doi.org/10.1371/journal.pclm.0000014.g010

both studies are known to respond quickly to changes in ocean conditions and given our assumption that the surveys are consistently sampling at the right time and location to fully characterize the short-term response.

While our study did not detect a shift in community state in the southern and central CCE during the 2014–2016 heatwave, we did detect a shift in the 1960s. The 1960s shift was likely due to a regime shift previously detected in the southern California ichthyoplankton

community [7]. The Peabody et al. [7] study included a much broader suite of ichthyoplankton species than our study which limits our ability to evaluate whether the species driving the shifts are consistent among studies. Previous studies have also documented a shift in response to the 1976/1977 PDO shift (e.g., [7, 68]), but our analyses did not. Our estimated biology trend is consistent with the evidence of this regime shift, however, only ichthyoplankton time series are available prior to the 1970s and there are gaps in the ichthyoplankton data from the late 1960s through the 1970s. The trend estimate therefore has higher uncertainty during this period than elsewhere in the time series.

The CCE biology time series included in this study showed strong coherence in community signal in response to regional climate perturbations. Although they span across multiple trophic levels, life-history strategies, and datasets, most of the biological time series loaded in the same direction on the shared trend (Fig 6). In addition, our the CCE shared biology trend and loadings captured an unusual aspect of the 2014–2016 warming events: the abundance of several taxa, including young-of-year rockfish and anchovy, was high during the marine heatwave [22, 29, 31]. By contrast, their abundance was greatly reduced in most previous warm events, including two of the strongest El Niño events on record (1982–1983, 1997–1998) and unusually low productivity conditions (2005–2006) [69]. High abundances of young-of-year rockfish and groundfish, squid, and krill in the CCE are generally associated with more southward transport and subarctic source waters, while abundances are typically far lower in years with more subtropical waters, which are often associated with El Niño and anomalous warm events [29, 70]. The unexpectedly high abundance of these taxa in 2014–2016, despite surface-oriented marine heatwave, may be related to the prevalence of subsurface waters that were more subarctic than subtropical in origin [29] and to some concurrent strong upwelling events, particularly in spring 2015 [71, 72].

Our results were consistent with recent studies of several top predators in the CCE. The DFA trends and loadings indicate a negative response of sea lion pup growth and weight to the 2014–2016 marine heatwave, which also aligns with past work showing that sea lion pup condition covaries with abundance of forage such as larval anchovy and sardine, which provide quality prey to sustain lactation in nursing mothers [73]. Pup condition also improved at the tail end of the marine heatwave when, despite the warm water, anchovy abundance increased dramatically [31]. The trends and loadings suggest that the reproductive success of some seabirds in the central CCE was not diminished by the heatwave, although the heatwave had severe impacts seabird productivity in regions to the north [20].

Regional comparison of the marine heatwave's effect on community state

A compelling outcome of our analysis and a similar analysis applied to Alaskan species by Litzow et al. [42] is that neither detected state changes in North Pacific communities following the massive 2014–2016 marine heatwave, despite the extremely anomalous physical conditions throughout most of the basin and a litany of concurrent biological, ecological, social and economic effects (see Introduction). An important characteristic of both studies is the temporal scale of community analysis (1972–2017 for the Gulf of Alaska (GOA) and 1951–2017 for the CCE). This long temporal scale provides an important context for comparing contemporary change with the magnitude of historical community shifts. In addition, the Bayesian DFA accounts for uncertainty in the shared trends in a way that prevents premature detection of wholesale ecosystem shifts.

We note that Suryan et al. [74], fitted a single-trend, non-Bayesian DFA model to a larger set of GOA biological time series (n = 187) over a shorter time span (2010–2018) and found evidence of a well-resolved shift that implied different community states during 2010–2014

and 2015–2018. The different conclusions of Suryan et al. [74] and Litzow et al. [42] studies speak to an inherent tension in retrospective analyses of community change. Limited time series availability means that analyses can be taxonomically and functionally broad (e.g., [74]), or temporally extensive (e.g., [42]), but not both. Each approach has advantages, but direct comparison between the two is difficult. Given the impacts of the 2014–2016 event, and that long-term warming combined with marine heatwaves will push the CCE into novel climate states, we must consider ecological mechanisms that might explain why these communities were apparently resilient to the marine heatwave, along with revisiting methodological details that could further clarify our results.

Environmental covariates

DFA models of CCE biology that included a climate covariate performed better than models without one. Nitrate flux into the surface mixed layer (BEUTI) was the best-performing covariate for individual species in addition to the shared trend in the southern and central CCE over the past three decades. Nitrate flux had a strong positive effect on the abundance of krill and some larval fishes and on the reproductive success of seabirds, and a moderate positive effect on some pelagic juvenile fishes, squid, and sea lion pup births. Stronger upwelling magnitude (CUTI), which is correlated with nitrate flux, was the second-best predictor of community variability and had a positive albeit weaker effect on the same suite of species (S5 Fig). These findings are consistent with mechanistic understanding as upwelling increases the supply of nutrients to shallow waters and enhances the productivity at the lower trophic levels, including juvenile rockfishes [75], which affects foraging conditions for higher trophic level species, such as seabirds (e.g., [76]).

BEUTI and CUTI had a strong, negative correlations with juvenile/adult Pacific sardine and larval northern anchovy. The relative abundance of Pacific sardine in coastal waters off of Central California has been shown to be lower during periods of strong upwelling [70, 77]. This trend may reflect a change in the production of Pacific sardine or a shift in their relative distribution. In addition, a negative relationship between upwelling and sardine recruitment can generally be explained by the transfer of fish larvae to offshore areas where they have low chance of survival during periods of strong equatorward flow and upwelling [78, 79]. Our understanding of the mechanisms driving anchovy population dynamics is limited [80].

Climate drivers often act in concert to influence community variability, and here we are evaluating the effects of climate variables one at a time. An important next step of this work will be to examine whether including multiple climate covariates further improves the forecast skill of the CCE biology and our community state indicator. However, the individual climate variables are collinear and share information, which affects our ability to makes inference on the covariates. Furthermore, our study is broad synthesis of community indicators and their response to climate perturbations, and should not be interpreted as replacing more detailed investigations into the drivers and mechanistic understanding of the indicators included here.

Community state forecasting skill

Our approach for creating simultaneous predictions of species responses and shared ecosystem variability to ocean conditions shows promise for developing near-term forecasts of community state. Our forecasts are based on outputs from the CCE ROMS, which have been used to examine how oceanographic processes affect fish recruitment variability [81, 82] and productivity [83], species habitat suitability [84, 85], and species spatial distributions [86, 87]. The CCE ROMS also supports nowcasts of species distributions based on observed ocean conditions [88–90]. Moreover, multiple efforts are underway in the CCE and other coastal systems

to use ROMS outputs to develop short-term forecasts of ocean conditions for uptake by scientists, managers, and other end-users [35, 91–93]. Here, we were able to create forecasts of community state and several individual species parameters one year in advance based on observations of a single climate variable (nitrate flux). Forecast lead times could be extended further by using forecasts of ocean conditions rather than observed conditions, and ocean temperatures in the CCE can be skillfully forecast months to a year in advance, with particularly high skill in the late winter and spring [94]. Future extensions of our work will evaluate whether different combinations of climate variables and time lags might improve our forecasting skill.

Using DFA to forecast attributes of community structure in the CCE allows us to create simultaneous forecasts of trends, or 'ecosystem state', and raw time series. Our approach could also be applied individually to each dataset in our analysis to generate taxa-specific indicators (e.g., seabird productivity, juvenile fish abundance), though these forecasts would be expected to differ from those with the entire CCE dataset. Similarly, if ecosystem states were not a focus of inference, alternative forecast models could be applied (e.g., ARIMA or non-parametric models) [67]. Forecasts for individual time series from the DFA models used here can be seen as a mixture of the AR forecast on the estimated trends (Fig 9), and linear effects of forecasted climate variables on each time series (Fig 8). Species that have strong associations or loadings on the trend and estimated climate effects that are large in magnitude (e.g., market squid, Pacific sanddabs, shortbelly rockfish *Sebastes jordani*) are expected to have the most accurate predictions, while those species with weak loadings and weaker effects of climate variables (e.g., California smoothtongue (*Leuroglossus stilbius*) are expected to have poorer forecast performance.

Nonstationary relationships are an important consideration for producing reliable ecological forecasts. While the year-to-year variability in the estimated trend did appear to be stationary in our community models (Figs 5 and 9), the autocorrelation appeared to be nonstationary with the lag-1 autocorrelation between 2000–present being significantly higher (0.82) than over the years 1981–2000 (0.23). In addition to nonstationary variance parameters, future analyses may also consider nonstationary relationships in the covariate relationships, or potential interactions between covariates. A growing number of retrospective analyses have revealed nonstationary relationships among climate and individual species or community-level variables [42, 95–99]. In the northeast Pacific Ocean, these studies have been mostly focused on Alaskan ecosystems with long time series describing climate and biological processes. The best-documented instance of nonstationary relationships among climate and biology time series in the North Pacific centers on a climate shift in the late 1980s [98]. Decades of observational data on either side of that event allow for statistically robust tests for nonstationarity that are not yet available for post-2014–2016 conditions. However, early indications from Alaska suggest the possibility that long-standing relationships between leading climate modes and individual climate and biology time series may have changed following 2014 [99].

Management application

Our approach for developing a community state indicator to track and predict the response of marine ecosystems to climate perturbations has the potential to support ecosystem-based and climate-ready management in multiple ways. Garnering knowledge of community state and the potential for large shifts in ecosystem structure in response to intense and novel climate perturbations can help inform better, more rapid management decisions for mitigating ecological and socioeconomic impacts. Our intention is to continually update our analyses when new data become available to provide the most up-to-date information on the CCE community state for scientists, managers, and stakeholders.

The combination of long-term monitoring surveys and data with the modeling framework we advance here can also help scientists identify or refine key variables of ecosystem change that are summarized for ecosystem assessments in support of decision-making [32]. For example, it might be prudent to emphasize ecological time series that load strongest on ecosystem state trends and demonstrate strong, predictable relationships with climate variables (or other covariates of interest) over time series with weaker loadings or lower forecast skill. Furthermore, our approach can provide valuable ecosystem information for scientific, management and coastal communities during times when researchers cannot sample the biology in marine ecosystems. This added value became acutely apparent in 2020 when myriad ocean surveys were cancelled or limited in spatiotemporal scope due to safety restrictions associated with the COVID-19 pandemic.

Finally, our approach provides a quantitative way to help managers discern short-term periods of unusual community dynamics and/or high variability—such as the 2014–2016 marine heatwave—from state shifts that represent more enduring transitions into new regimes of ecosystem structure or productivity. Given that global climate change is expected to amplify ocean change, approaches like the one applied here will become increasingly valuable for identifying novel community states that require new marine resource management and conservation considerations.

Supporting information

S1 Appendix. Standardization of time series from spatially resolved datasets.
(PDF)

S1 Table. Climate and biology time series included in the study analyses. A list of climate and biology time series included in the analyses and the associated units of measurements, data transformations (if applicable), years of data, and data sources. [1]UCSC ROMS model, [2]NOAA Marine Mammal Lab, [3]Point Blue / USFW, [4]CalCOFI, [5]NOAA Rockfish Recruitment & Ecosystem Assessment Survey.
(PDF)

S2 Table. Summary information for the Bayesian DFA biology-covariate one-trend candidate models and the top two biology only models (years 1981–2017). Only one trend models are shown because they outperformed all two and three trend models. The table indicates whether process error was estimated, the number of model trends, estimated log predicted densities (ELPD), standard error of ELPD, and the environmental covariate included in model. All models had an AR(1) coefficient on the trend and Student-t deviations.
BEUTI = Biologically Effective Upwelling Transport Index; CUTI = Coastal Upwelling Transport Index; ILD = Isothermal Layer Depth; SST = Sea Surface Temperature; BV = Brunt-Väisälä frequency; SSH = Sea Surface Height.
(PDF)

S3 Table. Observations, predictions, and prediction errors for single species parameters in 2018. The predictions and errors were derived from the top four biology-covariate models shown in Table 2. Species with the lowest prediction errors are highlighted in bold.
(PDF)

S1 Fig. Climate and biology time series used in the study analyses. The time series include climate indices (gray), ichthyoplankton abundance indices (orange), seabird reproductive success (teal), juvenile fishes and invertebrates (blue), and California sea lion pup parameters. Time series are scaled by their mean and standard deviation.
(PDF)

S2 Fig. AR(1) coefficient on the southern/central California latent climate trend.
(PDF)

S3 Fig. The Student-t deviations degrees of freedom parameter (nu) in the southern/central California climate trend. This figure demonstrates support for a heavy-tailed deviations of the latent trend. Smaller values of the degrees of freedom parameter (e.g., less than 10 or 20) are consistent with heavy-tailed deviations.
(PDF)

S4 Fig. The Student-t deviations degrees of freedom parameter (nu) in the southern/central California biology trend.
(PDF)

S5 Fig. A summary of the effect of the Cumulative Upwelling Transport Index (CUTI) on the individual single species parameter included in the DFA analyses. Cal. = California, Juv. = juvenile fish stage, Juv./adult = juvenile and adult stages combined, all other fish are larval fish. Blue error bars reflect 95% credible intervals.
(PDF)

S6 Fig. A summary of the effect of the Isothermal Layer Depth (ILD) on the individual single species parameter included in the DFA analyses. Cal. = California, Juv. = juvenile fish stage, Juv./adult = juvenile and adult stages combined, all other fish are larval fish. Blue error bars reflect 95% credible intervals.
(PDF)

S7 Fig. A summary of the effect of the sea surface temperature on the individual single species parameter included in the DFA analyses. Cal. = California, Juv. = juvenile fish stage, Juv./adult = juvenile and adult stages combined, all other fish are larval fish. Blue error bars reflect 95% credible intervals.
(PDF)

S8 Fig. Community variability in the southern California Current ecosystem (1981–2018). Posterior distributions for loadings on individual time series associated with the biology trend in Fig 9 are shown. Only time series with $\geq$ 90% of loading distributions above or below zero are shown. Loadings with darker shading indicate time series loading most strongly on the biology trend. See S1 Table for times series details.
(PDF)

S9 Fig. Fitted values for biology-covariate model including BEUTI (nitrate flux) as a covariate (1981–2017). Blue circles = observations; blue line = fitted model, red circles = 2018 observations; red triangles = model predictions of single species parameters in 2018. Fish life stages: L = larval, J = juvenile, A = adult. 2018 observations were not available for juvenile northern anchovy.
(PDF)

S10 Fig. (S9 Fig continued) Fitted values for biology-covariate model including BEUTI (nitrate flux) as a covariate (1981–2017). Blue circles = observations; blue line = fitted model, red circles = 2018 observations; red triangles = model predictions of single species parameters in 2018. Fish life stages: L = larval, J = juvenile, A = adult. 2018 observations were not available for juvenile northern anchovy.
(PDF)

S11 Fig. Coefficient of variation (CV) and log CV of 2018 predictions of individual species parameters plotted against the mean and log CV of loadings related to each species, respectively, and the mean and log CV of coefficients relating each species to BEUTI (nitrate flux), respectively.
(PDF)

Acknowledgments

We thank those who have spent countless hours planning field surveys and collecting data for the invaluable time series used in our study. We thank the U.S. Fish and Wildlife Service for granting permission and providing resources to conduct research on the Farallon Islands National Wildlife Refuge. We thank B. Feist for creating the map of the sampling areas (Fig 1). We thank N. Tolimieri and T.L. Rogers for their helpful comments on an earlier version of this manuscript.

Author Contributions

Conceptualization: Mary E. Hunsicker, Eric J. Ward, Michael A. Litzow, Sean C. Anderson, Chris J. Harvey, Jin Gao.

Data curation: John C. Field, Michael G. Jacox, Sharon Melin, Andrew R. Thompson, Pete Warzybok.

Formal analysis: Mary E. Hunsicker, Eric J. Ward.

Funding acquisition: Mary E. Hunsicker, Eric J. Ward, Michael A. Litzow, Chris J. Harvey.

Methodology: Eric J. Ward, Sean C. Anderson, Jin Gao.

Project administration: Mary E. Hunsicker, Michael A. Litzow.

Software: Mary E. Hunsicker, Eric J. Ward, Michael A. Litzow, Sean C. Anderson.

Visualization: Mary E. Hunsicker, Eric J. Ward, Sean C. Anderson.

Writing – original draft: Mary E. Hunsicker, Eric J. Ward, Michael A. Litzow.

Writing – review & editing: Mary E. Hunsicker, Eric J. Ward, Michael A. Litzow, Sean C. Anderson, Chris J. Harvey, John C. Field, Jin Gao, Michael G. Jacox, Sharon Melin, Andrew R. Thompson, Pete Warzybok.

References

1. Hobday AJ, Oliver ECJ, Sen Gupta A, Benthuysen JA, Burrows MT, Donat MG, et al. Categorizing and naming marine heatwaves. Oceanography 2018; 31: 162–173.
2. Sen Gupta A, Thomsen M, Benthuysen JA, Hobday AL, Oliver E, Alexander LV, et al. Drivers and impacts of the most extreme marine heatwaves events. Sci. Rep. 2020; 10: 19359. https://doi.org/10.1038/s41598-020-75445-3 PMID: 33168858
3. Beaugrand G, Edwards M, Brander K, Luczak C, Ibanez F. Causes and projections of abrupt climate-driven ecosystem shifts in the North Atlantic. Ecol. Lett. 2008; 11: 1157–1168. https://doi.org/10.1111/j.1461-0248.2008.01218.x PMID: 18647332
4. Beaugrand G, Conversi A, Chiba S, Edwards M, Fonda-Umani S, Greene C, et al. Synchronous marine pelagic regime shifts int he Northern Hemisphere. Phil. Trans. R. Soc. 2015; 370: 20130272. https://doi.org/10.1098/rstb.2013.0272
5. Möllmann C, Diekmann R. Marine Ecosystem Regime Shifts Induced by Climate and Overfishing: A Review for the Northern Hemisphere. Adv. Ecol. Res. 2012; 47: 303.347.

6. Wernberg T, Bennett S, Babcock RC, De Bettignies T, Cure K, Depczynksi M, et al. Climate-driven regime shift of a temperate marine ecosystem. Science 2016; 353: 169–172. https://doi.org/10.1126/science.aad8745 PMID: 27387951

7. Peabody CE, Thompson AR, Sax DF, Morse RE, Perretti CT. Decadal regime shifts in southern California's ichthyoplankton assemblage. Mar. Ecol. Prog. Ser. 2018; 607: 71–83.

8. Benson AJ, Trites AW. Ecological effects of regime shifts in the Bering Sea and eastern North Pacific Ocean. Fish Fish. 2002; 3: 95–113.

9. Hare SR, Mantua NJ. Empirical evidence for North Pacific regime shifts in 1977 and 1989. Prog. Oceanogr. 2000; 47: 103–145. https://doi.org/10.1016/s0079-6611(00)00033-1

10. Mantua NJ, Hare SR, Zhang Y, Wallace JM, Francis RC. A Pacific interdecadal climate oscillation with impacts on salmon production. Bull. Am. Meteorol. Soc. 1997; 78, 1069–1079.

11. Anderson PJ. Piatt JF. Community reorganization in the Gulf of Alaska following ocean climate regime shift. Mar. Ecol. Prog. Ser. 1999; 189: 117–123.

12. Litzow MA, Ciannelli L. 2007. Oscillating trophic control induces community reorganization in a marine ecosystem. Ecol. Lett. 2007; 10: 1124–1134. https://doi.org/10.1111/j.1461-0248.2007.01111.x PMID: 17883409

13. Bond NA, Cronin MF, Freeland H, Mantua N. Causes and impacts of the 2014 warm anomaly in the NE Pacific. Geophys. Res. Lett. 2015; 42, 3414–3420. https://doi.org/10.1002/2015GL063306

14. Walsh JE, Thoman RL, Bhatt US, Bieniek PA, Brettschneider B, Brubaker M, et al. The high latitude heat wave of 2016 and its impacts on Alaska. Bull. Am. Meteorol. Soc. 2018; 99: S39–S43. https://doi.org/10.1175/BAMS-D-17-0105

15. Jacox MG, Alexander MA, Mantua NJ, Scott JD, Hervieux G, Webb RS, et al. Forcing of multiyear extreme ocean temperatures that impacted California Current living marine resources in 2016. Bull. Am. Meteorol. Soc. 2018a; 99: S27–S33. https://doi.org/10.1175/BAMS-D-17-0119.1

16. Laufkötter C, Zscheischler J, Frölicher TL. High-impactmarine heatwaves attributable to human-induced global warming. Science 2020; 369: 1621–1625. https://doi.org/10.1126/science.aba0690 PMID: 32973027

17. Cavole LM, Demko AM, Diner RE, Giddings A, Koester I, Pagniello CM, et al. Biological impacts of the 2013–2015 warm-water anomaly in the Northeast Pacific: winners, losers, and the future. Oceanography 2016; 29, 273–285.

18. Santora JA, Mantua NJ, Schroeder ID, Field JC, Hazen E, Bograd SJ, et al. Habitat compression and ecosystem shifts as potential links between marine heatwave and record whale entanglements. Nat. Commun. 2020; 11: 1–12. https://doi.org/10.1038/s41467-019-13993-7 PMID: 31911652

19. Jones T, Parish JK, Peterson WT, Bjorkstedt EP, Bond NA, Balance LT, et al. Massive mortality of a planktivorous seabird in response to a marine heatwave. Geophys. Res. Lett. 2018; 45: 3193–3202.

20. Piatt JF, Parrish JK, Renner HM, Schoen SK, Jones TT, Arimitsu ML, et al. Extreme mortality and reproductive failure of common murres resulting from the northeast Pacific marine heatwave of 2014–2016. PLoSONE 2020; 15: e0226087. https://doi.org/10.1371/journal.pone.0226087 PMID: 31940310

21. McCabe RM, Hickey BM, Kudela RM, Lefebvre KA, Adams NG, Bill BD, et al. An unprecedented coast-wide toxic algal bloom linked to anomalous ocean conditions. Geophys. Res. Lett. 2016; 43: 10366–10376. https://doi.org/10.1002/2016GL070023 PMID: 27917011

22. Santora JA, Hazen EL, Schroeder ID, Bograd SJ, Sakuma KM, Field JC. Impacts of ocean climate variability on biodiversity of pelagic forage species in an upwelling ecosystem. Mar. Ecol. Prog. Ser. 2017; 580: 205–220.

23. Brodeur RD, Auth TD, Phillips AJ. Major shifts in pelagic micronekton and zooplankton community structure in an upwelling ecosystem related to an unprecedented marine heatwave. Front. Mar. Sci. 2019. https://doi.org/10.3389/fmars.2019.00212

24. Nielsen JM, Rogers LA, Brodeur RD, Thompson AR, Auth TD, Dreary AL, et al. Responses of ichthyoplankton assemblages to the recent marine heatwave and previous climate fluctuations in several Northeast Pacific marine ecosystems. Glob. Chang. Biol. 2020; 27: 506–520. https://doi.org/10.1111/gcb.15415 PMID: 33107157

25. Sakuma KM, Field JC, Mantua NJ, Ralston S, Marinovic BB, Carrion CN. Anomalous epipelagic micronekton assemblage patterns in the neritic waters of the California Current in spring 2015 during a period of extreme ocean conditions. CalCOFI Reports 2016; 57: 163–183.

26. Morgan CA, Beckman BR, Weitkamp LA, Fresh KL. Recent ecosystem disturbance in the Northern California Current. Fisheries 2019; 44: 465–474. https://doi.org/10.1002/fsh.10273

27. Sanford E, Sones JL, García-Reyes M, Goddard JH, Largier JL. Widespread shifts in the coastal biota of northern California during the 2014–2016 marine heatwaves. Sci. Rep. 2019; 9: 1–14. https://doi.org/10.1038/s41598-018-37186-2 PMID: 30626917

28. Walker HJ Jr, Hastings PA, Hyde JR, Lea RN, Snodgrass OE, Bellquist LF. Unusual occurrences of fishes in the Southern California Current System during the warm water period of 2014–2018. Estuar. Coast. Shelf Sci. 2020; 236: 106634.

29. Schroeder ID, Santora JA, Bograd SJ, Hazen EL, Sakuma KM, Moore AM, et al. Source water variability as a driver of rockfish recruitment in the California Current Ecosystem: implications for climate change and fisheries management. Can. J. Fish. Aquat. Sci. 2019; 76: 950–960. https://doi.org/10.1139/cjfas-2017-0480

30. Field JC, Miller RA, Santora JA, Tolimieri N, Haltuch MA, Brodeur RD, et al. Spatiotemporal patterns of variability in the abundance and distribution of winter-spawned pelagic juvenile rockfish in the California Current. PloS one 2021; 16: e0251638. https://doi.org/10.1371/journal.pone.0251638 PMID: 34043656

31. Thompson AR, Schroeder ID, Bograd SJ, Hazen EL, Jacox MG, Leising AL, et al. State of the California Current 2018–19: a novel anchovy regime and a new marine heatwave? CalCOFI Reports 2019; 60: 1–65.

32. Harvey CJ, Fisher J, Samhouri JF, Williams GD, Francis TB, Jacobson KC, et al. The importance of long-term ecological time series for integrated ecosystem assessment and ecosystem-based management. Prog. Oceanogr. 2020. https://doi.org/10.1016/j.pocean.2019.102234 PMID: 33184522

33. Hobday AJ, Spillman CM, Paige Eveson J, Hartog JR. Seasonal forecasting for decision support in marine fisheries and aquaculture. Fish. Oceanogr. 2016; 25: 45–56.

34. Tommasi D, Stock CA, Hobday AJ, Methot R, Kaplan IC, Eveson JP, et al. Managing living marine resources in a dynamic environment: the role of seasonal to decadal climate forecasts. Prog. Oceanogr. 2017; 152: 15–49.

35. Jacox MG, Alexander MA, Siedlecki S, Chen K, Kwon Y-O, Brodie S, et al. Seasonal-to-interannual prediction of North American coastal marine ecosystems: Forecast methods, mechanisms of predictability, and priority developments. Prog. Oceanogr. 2020. https://doi.org/10.1016/j.pocean.2019.102234 PMID: 33184522

36. Koslow JA, Hobday AJ, Boehlert GW. Climate variability and marine survival of coho salmon (*Oncorhynchus kisutch*) in the Oregon production area. Fish. Oceanogr. 2002; 11: 65–77.

37. Koslow J, Goericke R, Watson W. Fish assemblages in the Southern California Current: relationships with climate, 1951–2008. Fish. Oceanogr. 2013; 22: 207–219.

38. Planque B, Arneberg P. Principal component analyses for integrated ecosystem assessments may primarily reflect methodological artefacts. ICES J. Mar. Sci. 2018; 75: 1021–1028.

39. Zuur AF, Tuck ID, Bailey N. Dynamic factor analysis to estimate common trends in fisheries time series. Can. J. Fish. Aquat. Sci. 2003; 60: 542–552.

40. Ward EJ, Anderson SC, Damiano LA, Hunsicker ME, Litzow MA. Modeling regimes with extremes: the bayesdfa package for identifying and forecasting common trends and anomalies in multivariate time-series data. R J 2019; 11: 46–55.

41. Anderson SC, Branch TA, Cooper AB, Dulvy NK. Black-swan events in animal populations. Proc. Natl. Acad. Sci. U.S.A. 2017; 114: 3252–3257. https://doi.org/10.1073/pnas.1611525114 PMID: 28270622

42. Litzow MA, Hunsicker ME, Ward EJ, Anderson SC, Gao J, Zador S, et al. Evaluating ecosystem change as Gulf of Alaska temperature exceeds the limits of preindustrial variability. Prog. Ocean. 2020a; 117: 7665–7671.

43. Neveu E, Moore AM, Edwards CA, Fiechter J, Drake P, Jacox MG, et al. A historical analysis of the California Current using ROMS 4D-Var. Part I: System configuration and diagnostics, Ocean Model. 2016; 99: 133–151. https://doi.org/10.1016/j.ocemod.2015.11.012

44. Jacox MG, Edwards CA, Hazen EL, Bograd SJ. Coastal upwelling revisited: Ekman, Bakun, and improved upwelling indices for the U.S. west coast. J. Geophys. Res. 2018b. https://doi.org/10.1029/2018JC014187

45. Checkley DM Jr, Barth JA. Patterns and processes in the California Current System. Prog. Ocean. 2009; 83, 49–64.

46. Gottscho AD. Zoogeography of the San Andreas Fault system: Great Pacific Fracture Zones correspond with spatially concordant phylogeographic boundaries in western North America. Biological Reviews 2016; 91: 235–254. https://doi.org/10.1111/brv.12167 PMID: 25521005

47. Jacox MG, Fietcher J, Moore AM, Edwards CA. ENSO and the California Current coastal upwelling response. J. Geophys. Res. 2015. https://doi.org/10.1002/2014JC010650

48. Schroeder ID, Santora JA, Moore AM, Edwards CA, Fietcher J, Hazen EL, et al. Application of a data assimilative regional ocean modeling system for assessing California Current System ocean conditions, krill, and juvenile rockfish interannual variability. Geophys. Res. Lett. 2014; 41: 5942–5950. https://doi.org/10.1002/2014GL061045

49. Amante C, Eakins BW. ETOPO1 1 Arc-Minute Global Relief Model: Procedures, Data Sources and Analysis. NESDIS NGDC-24, National Geophysical Data Center, United States Department of Commerce, Boulder, CO, March 2009. 19 p. https://doi.org/10.7289/V5C8276M

50. McClatchie S, Duffy-Anderson J, Field JC, Goericke R, Griffith D, Hanisko DS, et al. Long time series in US fisheries oceanography. Oceanography 2014; 27: 48–67.

51. Stan Development Team. RStan: The R interface to Stan. 2018.

52. R Core Team. R: A language and environment for statistical computing. R Foundation for Statistical Computing, Vienna, Austria, 2021.

53. Ward EJ, Anderson SC, Damiano LA, Malick MJ. bayesdfa: Bayesian Dynamic Factor Analysis (DFA) with 'Stan'. R package version 1.1.0 2020. https://CRAN.R-project.org/package=bayesdfa.

54. Holmes EE, Ward EJ, Scheuerell MD. Analysis of multivariate time series using the MARSS package; 2018.

55. Anderson SC, Ward EJ. Black swans in space: modelling spatiotemporal processes with extremes. Ecology 2019; 100: e02403. https://doi.org/10.1002/ecy.2403 PMID: 29901233

56. Hoffman MD, Gelman A. The No-U-Turn Sampler: Adaptively Setting Path Lengths in Hamiltonian Monte Carlo. J. Mach. Learn. Res. 2014; 15: 1593–1623.

57. Carpenter B, Gelman A, Hoffman MD, Lee D, Goodrich B, Betancourt M, et al. Stan: A Probabilistic Programming Language. J. Stat. Softw. 2017. https://doi.org/10.18637/jss.v076.i01

58. Gelman A, Rubin DB. Inference from Iterative Simulation Using Multiple Sequences. Statist. Sci. 1992; 7: 457–472.

59. Gelman A, Carlin JB. Stern HS, Dunson DB, Vehtari A, Rubin DB. Bayesian Data Analysis. 3rd ed. CRC Press; 2013.

60. Bürkner P-C, Gabry J, Vehtari A. Approximate leave-future-out cross-validation for Bayesian time series models. J. Stat Comput. Simul. 2020; 90: 2499–2523.

61. Vehtari A, Gelman A, Gabry J. Practical Bayesian model evaluation using leave-one-out cross-validation and WAIC. Statistics and Computing 2017; 27: 1413–1432. https://doi.org/10.1007/s11222-016-9696-4

62. Seo H, Brink KH, Dorman E, Koracin D, Edwards CA. What determines the spatial pattern in summer upwelling trends on the US West Coast? J. Geophys. Res. Oceans 2012. https://doi.org/10.1029/2012JC008016

63. McClatchie S, Goericke R, Koslow JA, Schwing FB, Bograd SJ, Charter RW et al. The State of the California Current, 2007–2008: La Niña conditions and their effects on the ecosystem. Cal-COFI Rep. 2008; 49: 39–76.

64. McClatchie S, Goericke R, Schwing FB, Bograd SJ, Peterson WT, Emmett R, et al. The state of the California Current, 2008–2009: Cold conditions drive regional difference. CalCOFI Rep. 2009; 50: 43–68.

65. Bjorkstedt EP, Goericke R, McClatchie S, Weber E, Watson W, Lo N, et al. State of the California current 2009–2010: Regional variation persists through transition from the la Niña to el Niño (and back?). CalCOFI Rep. 2010; 51.

66. Holmes EE. Beyond theory to applications and evaluation: Diffusions approximations for population viability analysis. Ecol. Appl. 2004; 14: 1272–1293.

67. Ward EJ, Holmes EE, Thorson JT, Collen B. Complexity is costly: a meta-analysis of parametric and non-parametric methods for short-term population forecasting. Oikos 2014; 123: 652–661.

68. McGowan JA, Bograd SJ, Lynn RJ, Miller AJ. The biological response to the 1977 regime shift in the California Current. Deep Sea Res. II 2003; 50: 2567–2582.

69. Peterson WT, Emmett R, Goericke R, Venrick E, Mantyla A, Bograd S, et al. The State of the California Current, 2005–2006: warm in the north, cool in the south. CalCOFI Reports 2006; 47: 30–74.

70. Ralston S, Field JC, Sakuma KM. Long-term variation in a central California pelagic forage assemblage. J. Mar. Sys. 2015; 146: 26–37. https://doi.org/10.1016/j.jmarsys.2014.06.013

71. Peterson WT, Fisher JL, Strub PT, Du X, Risien C, Peterson J, et al. The pelagic ecosystem in the Northern California Current off Oregon during the 2014–2016 warm anomalies within the context of the past 20 years. J. Geophys. Res. 2017; 122: 7267–7290. https://doi.org/10.1002/2017jc012952 PMID: 33204583

72. Ryan JP, Kudela RM, Birch JM, Blum M, Bowers HA, Chavez FP, et al. Causality of an extreme harmful algal bloom in Monterey Bay, California, during the 2014–2016 northeast Pacific warm anomaly. Geophys. Res. Lett. 2017; 44: 5571–5579. https://doi.org/10.1002/2017GL072637

73. McClatchie S, Field J, Thompson AR, Gerrodette T, Lowry M, Fiedler PC, et al. Food limitation of sea lion pups and the decline of forage off central and southern California. R. Soc. opensci. 2016; 3: 150628. https://doi.org/10.1098/rsos.150628 PMID: 27069651

74. Suryan RM, Arimitsu ML, Coletti HA, Hopcroft RR, Lindeberg MR, Barbeaux SJ, et al. Ecosystem response persists after a prolonged marine heatwave. Sci. Rep. 2021; 11: 6235. https://doi.org/10.1038/s41598-021-83818-5 PMID: 33737519

75. Ralston S, Sakuma KM, Field JC. Interannual variation in pelagic juvenile rockfish (Sebastes spp.) abundance—going with the flow. Fish. Ocean. 2013; 22:288–308. https://doi.org/10.1111/fog.12022

76. Wells BK, Field JC, Thayer JA, Grimes CB, Bograd SJ, Sydeman WJ, et al. Untangling the relationships among climate, prey and top predators in an ocean ecosystem. Mar. Ecol. Prog. Ser. 2008; 364: 15–29.

77. Santora JA, Schroeder ID, Field JC, Wells BK, Sydeman WJ. Spatiotemporal dynamics of ocean conditions and forage taxa reveals regional structuring of predator-prey relationships. Ecol. Appl. 2014; 24:1730–1747. https://doi.org/10.1890/13-1605.1 PMID: 29210234

78. Bailey KM, Francis RC. Recruitment of Pacific Whiting, Merluccius productus, and the ocean environment. Mar. Fish. Rev. 1985; 47: 8–11.

79. Nieto K, McClatchie S, Weber ED, Lennert-Cody CE. Effect of mesoscale eddies and streamers on sardine spawning habitat and recruitment success off Southern and central California, J. Geophys. Res. Oceans 2014; 119: 6330–6339, https://doi.org/10.1002/014JC010251

80. Sydeman WJ, Dedman S, Garcia-Reyes M, Thompson SA, Thayer JA, Bakun A, et al. Sixty-five years of northern anchovy population studies in the southern California Current: a review and suggestion for sensible management. ICES J. Mar. Sci. 2020; 77: 486–499.

81. Tolimieri N, Haltuch M, Lee Q, Jacox MG, Bograd SJ. Oceanographic drivers of sablefish recruitment in the California Current. Fish. Ocean, 2018; 27: 458–474, https://doi.org/10.1111/fog.12266

82. Haltuch MA, Tolimieri N, Lee Q, Jacox MG. Oceanographic drivers of petrale sole recruitment in the California Current Ecosystem, Fish. Ocean. 2020; 29:122–136. https://doi.org/10.1111/fog.12459

83. Siegelman-Charbit L, Koslow JA, Jacox MG, Hazen EL, Bograd SJ, Miller EF, et al. Physical forcing on fish abundance in the southern California Current System. Fish. Ocean. 2018; 27: 475–488. https://doi.org/10.1111/fog.12267

84. Abrahms B, Welch H, Brodie S, Jacox MG, Becker EA, Bograd SJ, et al. Dynamic ensemble models to predict distributions and anthropogenic risk exposure for highly mobile species. Divers. Distrib. 2019; 25: 1182–1193. https://doi.org/10.1111/ddi.12940

85. Cimino MA, Santora JA, Schroeder I, Sydeman W, Jacox MG, Hazen EL, et al. Essential krill species habitat resolved by seasonal upwelling and ocean circulation models within the large marine ecosystem of the California Current System. Ecography 2003; 43, 1–15. https://doi.org/10.1111/ecog.05204

86. Muhling B, Brodie S, Jacox MG, Snodgrass O, Dewar H, Tommasi D, et al. Dynamic habitat use of albacore and their primary prey species in the California Current System. CalCOFI Reports 2019; 60: 79–93.

87. Muhling B, Brodie S, Smith JA, Tommasi D, Gaitan CF, Hazen EL, et al. Predictability of species distributions deteriorates under novel environmental conditions in the California Current System. Front. Mar. Sci. 2020; https://doi.org/10.3389/fmars.2020.00589

88. Hazen EL, Palacios DM, Forney KA, Howell EA, Becker E, Hoover AL, et al. WhaleWatch: a dynamic management tool for predicting blue whale density in the California Current. J. Appl. Ecol. 2017. https://doi.org/10.1111/1365-2664.12820

89. Hazen EL, Scales KL, Maxwell SM, Briscoe D, Welch H, Bograd S, et al. A dynamic ocean management tool to reduce bycatch and support sustainable fisheries. Sci. Adv. 2018, 4: eaar3001. https://doi.org/10.1126/sciadv.aar3001 PMID: 29854945

90. Welch H, Hazen EL, Briscoe DK, Bograd SJ, Jacox MG, Eguchi T, et al. Environmental indicators to reduce loggerhead turtle bycatch offshore of Southern California. Ecol. Ind. 2019; 98: 657–664. https://doi.org/10.1016/j.ecolind.2018.11.001

91. Siedlecki SA, Kaplan IC, Hermann AJ, Nguyen TT, Bond NA, Newton JA, et al. Experiments with seasonal forecasts of ocean conditions for the northern region of the California Current upwelling system. Sci. Rep. 2016; 6: 27203. https://doi.org/10.1038/srep27203 PMID: 27273473

92. Kaplan IC, Williams GD, Bond NA, Hernmann AJ, Siedlecki S. Cloudy with a chance of sardines: forecasting sardine distributions using regional climate models. Fish. Oceanogr. 2016; 25: 15–2.

93. Malick M.J, Siedlecki SA, Norton EL, Kaplan IC, Haltuch MA, Hunsicker ME, et al. Environmentally driven seasonal forecasts of Pacific hake distribution. Front. Mar. Sci. 2020; 7: 578490. https://doi.org/10.3389/fmars.2020.578490

94. Jacox MG, Alexander MA, Stock CA, Hervieux G. On the skill of seasonal sea surface temperature forecasts in the California Current System and its connection to ENSO variability. Clim. Dyn. 2019; 53: 7519–7533.

95. Puerta P, Ciannelli L, Rykaczewski R, Opiekun M, Litzow MA. Do Gulf of Alaska fish and crustacean populations show synchronous non-stationary responses to climate? Prog. Oceanogr. 2019; 175: 161–170. https://doi.org/10.1016/j.pocean.2019.04.002

96. Litzow MA, Ciannelli L, Puerta P, Wettstein JJ, Rykaczewski RR, Opiekun M. Non-stationary climate–salmon relationships in the Gulf of Alaska. Proc. R. Soc. B Biol. Sci. 2018; 285: 20181855. https://doi.org/10.1098/rspb.2018.1855 PMID: 30404879

97. Litzow MA, Ciannelli L, Puerta P, Wettstein JJ, Rykaczewski RR, Opiekun M. Nonstationary environmental and community relationships in the North Pacific Ocean. Ecology 2019; 100: ecy.2760. https://doi.org/10.1002/ecy.2760 PMID: 31127608

98. Litzow MA, Hunsicker ME, Bond NA, Burke BJ, Cunningham CJ, Gosselin JL, et al. The changing physical and ecological meanings of North Pacific Ocean climate indices. Proc. Natl. Acad. Sci. U.S.A. 2020b; 117: 7665–7671. https://doi.org/10.1073/pnas.1921266117 PMID: 32205439

99. Litzow MA, Malick MJ, Bond NA, Cunningham CJ, Gosselin JL, Ward EJ. Quantifying a novel climate through changes in PDO-climate and PDO-salmon relationships. Geophys. Res. Lett. 2020c. https://doi.org/10.1029/2020GL087972